Applied Ocean Research 173 (2026) 105122

Contents lists available at ScienceDirect

Applied Ocean Research

journal homepage: www.elsevier.com/locate/apor

Review

Toward scalable and sustainable manufacturing solutions—A review of Large-Format Additive Manufacturing for marine applications with recommended methods and materials

Gianmaria Giannini [a,d,*], Giuseppe Giorgi [a], Giuliana Mattiazzo [a], Giovanni Avallone [b], Paulo Rosa-Santos [c,d], Francisco Taveira-Pinto [c,d]

[a] *Marine Offshore Renewable Energy Lab, Politecnico di Torino, Corso Duca degli Abruzzi 24, Torino, 10129, Italy*
[b] *Caracol - AM, Via Giovanni Amendola 25, Paderno Dugnano (MI), 20037, Italy*
[c] *Faculty of Engineering, University of Porto (FEUP), Rua Dr. Roberto Frias, s/n, Porto, 4200-465, Portugal*
[d] *CIIMAR – Interdisciplinary Centre of Marine and Environmental Research, Terminal de Cruzeiros do Porto de Leixões, Av. General Norton de Matos, s/n, Matosinhos, 4450-208, Portugal*

ARTICLE INFO

Keywords:
Marine renewable energy
Sustainable manufacturing
Marine structures
Thermoplastic composites
Circular economy
Smart manufacturing
3D printing pellet
Digital fabrication
Large Scale Additive Manufacturing
Large 3D-printing marine

ABSTRACT

Large-Format Additive Manufacturing (LFAM) presents a transformative opportunity for the marine sector, particularly in accelerating the development of emerging marine renewable energy technologies, which are often hindered by high capital and prototyping costs. LFAM enables the fabrication of complex, large-scale components with reduced tooling and lead times, offering potential cost reductions above 50% compared to conventional manufacturing methods. While LFAM is experiencing rapid adoption and standardisation in other industrial sectors, its transfer to marine engineering remains severely underexplored. The absence of a consolidated, marine-specific methodology currently bottlenecks the transition from prototyping to functional, industrial-scale production. The central motivation of this review is to bridge this critical gap. Therefore, this paper covers LFAM technologies, previous case studies on marine application, identifying suitable materials for the marine environment, and outlining key design and fabrication aspects. The study reviews the operational requirements, dimensions, and loads for MRE structures and small vessels within the context of LFAM. It critically analyses the hydrodynamic impact of surface roughness, differentiating between applications tolerant of as-printed finishes (e.g., wave energy converters) and high-Reynolds cases (e.g., tidal devices, planing vessels) where smoothing is essential to prevent performance degradation. A structured, seven-step methodology is proposed, encompassing material and technology selection, design approaches, printing strategy, post-processing, and certification. Additionally, specific energy and cost metrics are evaluated to support techno-economic assessments. The review and an overall critical analysis demonstrate the feasibility of LFAM for producing functional marine components. Key trends are identified, highlighting future research directions and immediate industrial applications, and laying the groundwork for scalable, cost-effective, and sustainable manufacturing solutions in the MRE and broader marine sectors.

Contents

* Corresponding author at: Marine Offshore Renewable Energy Lab, Politecnico di Torino, Corso Duca degli Abruzzi 24, Torino, 10129, Italy.
E-mail address: gianmaria.giannini@polito.it (G. Giannini).

https://doi.org/10.1016/j.apor.2026.105122
Received 22 January 2026; Received in revised form 20 May 2026; Accepted 27 May 2026
Available online 7 June 2026
0141-1187/© 2026 The Authors. Published by Elsevier Ltd. This is an open access article under the CC BY license (http://creativecommons.org/licenses/by/4.0/).

1. Introduction

The wider marine and offshore industry is facing increasing pressure to deliver efficient, sustainable, and cost-effective solutions for applications ranging from commercial vessels, marine renewable energy devices to hybrid structures. To ensure long-term sustainability and align with global climate goals, the maritime sector must embrace low-emission manufacturing processes, circularity, extended durability and recyclability of components, and ensuring responsible decommissioning.

Within this transformative context, the development of marine renewable energy (MRE) is increasingly recognised as a strategic priority. Besides, offshore wind, wave, and tidal energy systems are expected to play a central role in decarbonising the energy sector while supporting energy security and economic growth. In Europe, policy frameworks such as the EU Offshore Renewable Energy Strategy part of the broader 2050 long-term vision (European Commission, 2025) and national sectoral plans have been implemented to accelerate MRE deployment, streamline permitting, and foster innovation and supply chain (Ramos et al., 2021). However, to realistically implement these plans, marine systems — whether commercial vessels or MRE devices — require sustainable components that can withstand extreme environmental loads, high corrosive conditions, and continuous mechanical stress.

Marine systems, such as wind turbines (e.g. devices studied by Li et al., 2020; Díaz and Guedes Soares, 2020; Roga et al., 2022), tidal energy turbines (TED) (e.g. Clarke et al., 2007; Coiro et al., 2017; Alam et al., 2026) and wave energy converters (WECs) (e.g. Falcão, 2010; Babarit, 2015; Gao et al., 2020; Sirigu et al., 2020b; Giannini et al., 2021b, 2024, 2025; Pan et al., 2025), often feature complex and multi-functional geometries of their main structures and subcomponents. The need for robust yet lightweight materials has led to increased research into structural optimisation and manufacturing of high-performance parts such as blades and moving floaters. Moreover, complex structures such as wind and wave, multi-scope or multi-energy systems (Ramos et al., 2022; Clemente et al., 2023; Manolache and Andrei, 2024; Ahmed et al., 2025) highlight further design and manufacturing challenges spanning from high labour costs for construction and viable supply chain development.

Traditional marine manufacturing relies on intensive, often manual processes such as welding, casting, and machining (Gerwick, 2007), typically involving sequential construction and laborious fitting of components. While the introduction of glass-fibre reinforced plastic (GRP) improved weight and corrosion resistance (Shenoi et al., 2011), these composites are costly to fabricate, depend heavily on manual labour, and are not yet recyclable on a large scale (Gonçalves et al., 2022).

Furthermore, during manufacturing, classic GRP also poses health and environmental hazards due to dust and vapours (Abbate et al., 2006).

Large-Format Additive Manufacturing (LFAM) offers significant advantages over conventional manufacturing methods. Primarily, it enables zero-tooling production of large, complex parts and supports rapid prototyping, customisation, and integrated geometries (Caracol AM, 2026). For instance, thermoplastic LFAM makes possible the production of components, with typical weights and structural efficiencies similar to GRP, suitable for the marine environment. LFAM reduces lead times, minimises material waste, enables the use of recycled materials and supports digital data-driven, repeatable manufacturing, improving quality and potentially reducing costs. Furthermore, components created through LFAM can also be of complex shapes, reducing the number of overall structure's components and the need for assembly joints, thereby enhancing structure integrity.

Overall, LFAM for marine structures and components can allow the following potential added values:

- Light-weight structural-performing structures;
- Corrosion resistance to saltwater and extreme conditions;
- Low production costs for small number of items to be manufactured;
- Possibility of combining multiple parts in single components;
- Enable the fabrication of complex shapes.

To fully harness these structural and economic benefits, selecting the appropriate material family is paramount. Although cementitious LFAM is gaining traction for heavy static infrastructure (e.g., coastal defences and gravity-based foundations), such applications prioritise mass and compressive strength over geometric precision. In contrast, the design of dynamic marine systems — such as floating bodies and tidal turbine blades — demands high specific strength, strict buoyancy control, and tight tolerances (Sun et al., 2021). Consequently, this review focuses exclusively on polymer- and metal-based LFAM technologies. These materials offer the most immediate option for replacing traditional GRP and welded steel in the fabrication of hulls, superstructures, and active energy conversion modules, directly addressing the complex hydrodynamic and structural prerequisites for high-performance marine applications (Belvisi et al., 2024).

Despite its exponential growth and standardisation in other major industrial sectors, the application of LFAM in marine engineering remains fragmented and underexplored. Existing review papers typically address general or large-format AM without accounting for the unique requirements and harsh constraints of the marine environment (Moreno Nieto and Molina, 2020; Goh et al., 2024; Vanerio et al., 2024). Consequently, key stakeholders — including MRE developers, shipyards, and classification societies — lack a consolidated reference that addresses critical factors like the hydrodynamic impacts of surface roughness, techno-economic metrics, and structured guidelines and certification workflows.

This distinct lack of marine-specific guidelines creates a bottleneck in leveraging LFAM capabilities — such as design freedom, reduced tooling, and the use of recycled materials — which directly address high prototyping costs, extended lead times, and circular-economy requirements in MRE and small-vessel development. Therefore, the central motivation of this review is to explicitly address these gaps by systematically evaluating current LFAM technologies and materials for marine compatibility, encompassing endurance, fatigue performance, cost, and sustainability. By synthesising available scattered information into a practical methodology, the ultimate goal is to support informed decision-making and successfully align advanced manufacturing capabilities with the multi-disciplinary demands of the marine sector.

To explicitly address these gaps and establish a foundational, marine-specific methodology, the specific contributions of this review are to:

- map LFAM technologies against marine structural requirements;
- consolidate candidate polymer and metal material systems for marine exposure;
- propose a LFAM workflow for marine components; and
- introduce performance and cost metrics tailored to MRE and small vessels.

Ultimately, this review is intended as a practical reference for engineers planning MRE and vessel demonstrators, industrial partners evaluating LFAM against traditional GRP or steel fabrication, and regulatory bodies beginning to integrate additive manufacturing into marine certification rules.

Recent advancements in applied ocean research have heavily focused on optimising Marine Renewable Energy (MRE) devices, including novel wave energy converters (Ahmed et al., 2025; Zanuttigh et al., 2026; Salar et al., 2026; Okushemiya et al., 2026; Pan et al., 2025) and flapping-foil harvesters (Alam et al., 2026). LFAM is uniquely positioned as a critical enabler for the rapid development of such low Technology Readiness Level (TRL) technologies. Compared to conventional shipbuilding and offshore manufacturing techniques, LFAM might offer a highly efficient solution regarding life-cycle environmental costs, enable circular material economies, and present strong economic competitiveness for complex, one-off, or small-batch productions. Furthermore, it might provide unprecedented opportunities for decentralised production and significantly reduces the number of intermediate manufacturing steps.

Consequently, this review focuses exclusively on high-deposition-rate methodologies, such as polymer pellet extrusion and Wire Arc Additive Manufacturing (WAAM), as they uniquely satisfy the massive volumetric and structural demands typical of marine engineering. Conversely, conventional high-resolution approaches (e.g., filament-based AM or powder bed fusion) are distinctly disadvantageous due to severe build volume constraints and prohibitive scaling costs. The structured workflow proposed herein distinguishes itself from generic manufacturing frameworks by explicitly integrating marine-specific boundary conditions, namely extreme hydrodynamic loading, seawater exposure, and stringent classification society requirements.

To establish a logical narrative, this review is structured to systematically build towards a comprehensive, marine-specific manufacturing workflow and techno-economic assessment. Following Section 2 about Review Methodology, Section 3 provides the historical context and structural constraints motivating the adoption of LFAM in the maritime sector. Section 4 categorises the available LFAM technologies, while Section 5 identifies compatible polymer and metal material systems. Section 6 evaluates the critical hydrodynamic impacts of LFAM surface roughness, directly informing the seven-step implementation workflow detailed in Section 7. Finally, Section 8 establishes the techno-economic and energy metrics required to assess the viability of LFAM-focused marine projects, culminating in a discussion of future research priorities and conclusions in Sections 9 and 10, respectively.

2. Review methodology

To ensure a comprehensive and reproducible assessment of the current state of LFAM in marine applications, an integrative narrative review methodology was adopted. While this study does not strictly constitute a systematic review (e.g., PRISMA), the literature search, screening process, and thematic grouping were conducted following a structured approach to minimise selection bias and ensure a robust synthesis of the state-of-the-art.

2.1. Search strategy

The primary literature search was conducted using Google Scholar as the principal search engine, supplemented by targeted cross-referencing within major academic publisher databases (e.g., Elsevier, Springer, Taylor & Francis). The search strategy utilised Boolean combinations of primary keywords related to the manufacturing processes, the application domain, and material categories.

Core search strings for primary applications included: (*"Large-Format Additive Manufacturing" OR "LFAM"* OR *"Large Scale Additive Manufacturing"* OR *"LSAM"* OR *"Big Area Additive Manufacturing"* OR *"BAAM"* OR *"Wire Arc Additive Manufacturing"* OR *"WAAM"*) AND (*"marine"* OR *"offshore"* OR *"shipbuilding"* OR *"marine renewable energy"* OR *"MRE"* OR *"hydrodynamics"*).

Furthermore, to establish the current state-of-the-art and properly contextualise the specific literature gaps addressed by this paper, a dedicated secondary search was executed to identify existing review articles. This targeted search focused specifically on material classes and utilised strings such as: (*"review"*) AND (*"Large Format Additive Manufacturing"* OR *"LFAM"* OR *"Additive Manufacturing"* OR *"AM"*) AND (*"metals"* OR *"polymers"* OR *"thermoplastics"*).

The time span considered for the modern LFAM literature primarily ranged from 2014 to 2026, designed to capture the exponential growth and industrialisation of large-format printing technologies. Historical relevant first AM developments, foundational marine engineering, hydrodynamic texts dating back to 1950 were purposefully retained to establish the evolution of AM, marine materials and operational constraints.

2.2. Inclusion and exclusion criteria

To maintain the technical quality and relevance of the review, specific criteria were applied during the screening process.

- **Inclusion criteria:** (i) Peer-reviewed journal articles, major conference proceedings, and verified industrial case studies; (ii) publications explicitly reporting on material properties (focusing on polymers and metals), manufacturing scale, or marine environmental constraints; (iii) literature published by recognised international publishers to ensure rigorous peer review; and (iv) documents published in the English language.
- **Exclusion criteria:** (i) Purely conceptual papers lacking empirical data or detailed engineering frameworks; (ii) studies focusing exclusively on desktop-scale or micro-additive manufacturing (typically under 1 m^3 build volume) without clear scalability to marine applications; and (iii) non-peer-reviewed grey literature, with the explicit exception of established classification society standards (e.g., DNV, ABS, LR) and official manufacturer datasheets.

2.3. Screening process and risk of bias mitigation

The selection process followed a staged filtering approach. Initially, a broad title and abstract screening was performed to eliminate clearly out-of-scope papers. Subsequently, a full-text review was conducted on the retained articles to extract relevant data concerning structural loads, material performance, hydrodynamic impacts, and techno-economic metrics.

Given the narrative nature of this review, potential biases must be acknowledged. A reliance on English-language publications may exclude relevant regional developments, and there is an inherent publication bias favouring successful LFAM case studies over failed industrial implementations. To mitigate these risks, the review actively incorporated stringent classification society standards and critically evaluated the techno-economic limitations, fatigue challenges, and post-processing penalties of the technology, ensuring a balanced technological synthesis rather than a purely optimistic overview. The overall logic of the review process is schematised in Table 1.

Overall, approximately 5000 papers and documents were initially identified. Following the application of the exclusion criteria, roughly 2000 were retained for screening. From this subset, about 200 papers were ultimately selected for detailed analysis, categorisation, and data extraction based on their direct relevance to the specific scope of this review (e.g., LFAM marine structural applications, material durability, and hydrodynamic impacts). These selected studies constitute the core literature cited throughout this manuscript.

3. Background

3.1. Historical context and motivation

Throughout history, the nautical sector experienced various revolutions in terms of manufacturing and materials used. For millennia, manual manufacturing and wood were the uncontested options. At the end of this long period, following the industrial revolution, first full metal ships started to be produced. One of the first full metal ship was an iron steamship that crossed the English Channel from London to Paris in 1822. This ship sparked interest in the shipbuilding industry, as a result, supply chains were developed. As a consequence, increasingly larger ships such as the first ocean liners and warships were built.

More recently, composite materials have been adopted to fabricate boats to medium vessels — with first applications dating in early 1940s — demonstrating revolutionary performances in terms of weight, strength and resistance to corrosion. Fabrication methods evolved allowing relatively fast production bringing costs down, making possible affordable products for a wider public. A considerable number of military vessels made of GRP that varied by 10 to 80 m of length were produced starting from 1945, showing how GRP was a relevant alternative to metal vessels providing a series of advantages ranging from fuel-efficiency, speed and manoeuvring performances up to non-magnetic properties. In terms of civil applications, GRP have been employed for producing small boats, hovercrafts and catamarans. Especially in Japan, 60% of the fishing boats fleet was made by GRP. Nowadays, about 80% of the hulls of vessels up to 20 m are made by GRP (Rubino et al., 2020).

GRP is one of the larger family of composite materials, which typically consist of high-performance synthetic fibres — such as glass or carbon — embedded within a polymer matrix. The matrix, a thermosetting resin, undergoes a chemical curing process that results in a rigid, load-bearing structure. For the nautical sector, normally either, vinyl ester, polyester or epoxy resins are used. To achieve optimal structural strength and stiffness, high-performance fibres such as carbon or Kevlar can be incorporated into the composite layup. When combined with lightweight core materials, this configuration forms what is commonly referred to as a sandwich structure, offering enhanced mechanical performance while minimising weight.

The fabrication of such composites traditionally involves manual lay-up techniques, where fibre reinforcements are arranged in molds and impregnated with resin before curing. While effective, this process is labour-intensive, time-consuming, and often lacks repeatability, posing challenges for scalability and automation in marine manufacturing. The alignment of fibres influences the structural properties of the component. Therefore, composite-made components are typically anisotropic or orthotropic, meaning that their properties (like stiffness, strength, thermal expansion) vary depending on the direction of the fibres and reinforcement. Overall, traditional manufacturing methods rely heavily on manual labour, limiting design flexibility and increasing production time.

In brief, the evolution of marine manufacturing can be structured into four distinct waves: the millennia-long reliance on wood, the 19th-century transition to steel, and the mid-20th-century widespread adoption of GRP. Today, the industry is poised at the beginning of its logical "fourth wave" driven by LFAM. This new paradigm is underpinned by key enabling technologies such as game-changing pellet-fed polymer extrusion and WAAM. By shifting the manufacturing paradigm from labour-intensive, mold-dependent processes to digitally driven, automated, and near-net-shape fabrication, LFAM directly addresses

Table 1
Schematic of the integrative review process and thematic categorisation.

Review phase	Actions and outputs
1. Identification	Execution of core keyword strings across Google Scholar and major publisher databases. Targeted searches for LFAM/AM reviews focusing on metals and polymers. Focus on peer-reviewed literature (primarily 2015–2026).
2. Screening	Application of inclusion/exclusion criteria. Removal of desktop-scale AM studies and purely conceptual papers. Prioritisation of robust, data-backed engineering studies.
3. Extraction	Identification of representative quantitative data (e.g., Specific Energy Consumption (SEC) ranges, layer height (L_h) roughness parameters, mechanical fatigue limits).
4. Categorisation	Structuring the retained literature into five thematic clusters: (1) Technologies & Kinematics; (2) Polymer & Metal Materials; (3) Hydrodynamic Impacts; (4) The 7-Step Implementation Workflow; (5) Techno-Economic Metrics.

the modern demands for scalability, complex geometries, and rapid iteration. The main milestones prior to consolidating modern LFAM are depicted in the timeline shown in Fig. 1. The genesis of AM is widely attributed to 1986, when Charles Hull patented Stereolithography (SLA), introducing layer-by-layer photo-curing (Hull, 1986). Shortly after, in 1989, Scott Crump patented Fused Deposition Modelling (FDM), establishing the foundational principles of filament-based AM (Crump, 1992). Concurrently, the early 1990s witnessed the modern revival of WAAM at institutions such as Cranfield University, which built upon a 1925 welding patent to pioneer large-scale metal deposition (Ribeiro et al., 1996). The mid-1990s also saw the first experimental crossovers between polymer extrusion and metal, utilising Metal Injection Moulding (MIM) pellets as feedstock for fused deposition (Agarwala et al., 1996). For over a decade, polymer AM remained largely confined to desktop-scale volumes until 2000, when Materialise introduced the "Mammoth" SLA system. Utilising a novel curtain-recoating mechanism to bypass the fluid dynamics constraints of massive resin vats, Mammoth enabled the single-piece production of full-scale automotive prototypes (Materialise, 2020). In 2004, Khoshnevis (2004) introduced "Contour Crafting", demonstrating the feasibility of massive gantry systems for structural extrusion. Meanwhile, the democratisation of filament AM was catalysed in 2005 by Dr Adrian Bowyer's RepRap project, a community-based initiative that created open-source, self-replicating 3D printers and popularised the term Fused Filament Fabrication (FFF) (Jones et al., 2011). The defining milestone for modern LFAM, however, can be set to the year 2014. Through a cooperative research programme, Oak Ridge National Laboratory (ORNL) and Cincinnati Incorporated developed the, so called, Big Area Additive Manufacturing (BAAM) system. By replacing expensive filament with high-throughput polymer pellet extrusion, they drastically reduced material costs and increased deposition rates, culminating in the historic 2014 live printing of the "Strati" vehicle chassis—a project that permanently validated pellet LFAM for massive, functional engineering applications (Love et al., 2016; Duty et al., 2017).

3.2. Structural and regulatory constraints for LFAM adoption in marine systems

Marine structures installed in the ocean must be designed and manufactured to withstand significant environmental loads, including wind, marine currents and waves. Most critical loads are those due to waves. As illustrated in Fig. 2, extreme wave pressure values for various water depths in a Portuguese exposed ocean area (considered by Giannini et al., 2022) are presented, plotted over the Le Méhauté wave diagram (Le Méhauté, 1969). Depending on the wave theory applied, these pressures range from approximately 37 kPa at 5 m depth (typical design wave height $H_{peak} \approx 4$ m) to 340 kPa at 80 m depth (typical design wave height $H_{peak} \approx 30$ m). Wave loads on offshore structures may be further amplified by nonlinear phenomena (Wilson, 2003; Chakrabarti, 2005) such as sloshing, overtopping/wave run-up, slamming, wave breaking, pounding/resonance, and wave diffraction/reflection:

- **Sloshing:** This refers to the violent resonant oscillation of fluids within partially confined volumes, such as internal storage tanks or open moonpools. It induces high-magnitude dynamic pressures on container walls and can destabilise the vessel by altering its global dynamic response.
- **Wave run-up and overtopping:** Wave run-up describes the maximum vertical extent of water uprush against the hull. Overtopping occurs when this run-up exceeds the structure's freeboard, resulting in "green water" events—where solid masses of water inundate the deck or superstructure, imposing severe transient loads.
- **Slamming:** This describes the violent, impulsive impact of water against structural surfaces, characterised by extremely short-duration, high-intensity pressure peaks. It typically occurs during hull re-entry (bottom slamming) or rapid immersion of overhanging geometries (flare slamming), often inducing high-frequency structural vibrations known as whipping.
- **Wave breaking:** Breaking waves generate highly concentrated, impulsive hydrodynamic forces. When waves break directly against a structure (e.g., plunging breakers), the resulting shock pressures can be orders of magnitude higher than non-breaking wave loads, posing critical risks to local structural integrity.
- **Multi-body interaction and gap resonance:** In modular or closely spaced structures, fluid entrapment between floating bodies can lead to resonant wave amplification (gap resonance). These relative motions may result in structural collisions or "pounding" loads, leading to load amplification in confined gaps.
- **Diffraction and reflection:** These phenomena alter the incident wave field around large-volume structures. The interaction of incident and reflected waves can create localised areas of constructive interference (wave amplification) and high-frequency scattering, leading to pressure distributions that deviate significantly from undisturbed field predictions.
- **Coupled mooring dynamics:** For moored structures, non-linear restoring forces and low-frequency drift motions can lead to extreme tension peaks (snap loads) in mooring lines. These loads feed back into the hull dynamics, intensifying structural stress concentrations at attachment points.

Offshore structures span a range of applications, each with distinct design and manufacturing requirements. Conventional structures, primarily developed for the oil and gas industry, are typically very large and almost exclusively constructed from steel. Given the high margins in this sector, materials and methods are expected to remain unchanged, although there is a trend toward producing smaller sub-components using alternative materials such as GRF. Due to the significant costs associated with offshore installations, minimising and streamlining operations at sea is essential. When feasible, GRP components such as living modules are fabricated for direct installation offshore (Rubino et al., 2020), and similarly, suitable components may be produced via LFAM. There is a significant growing interest in the

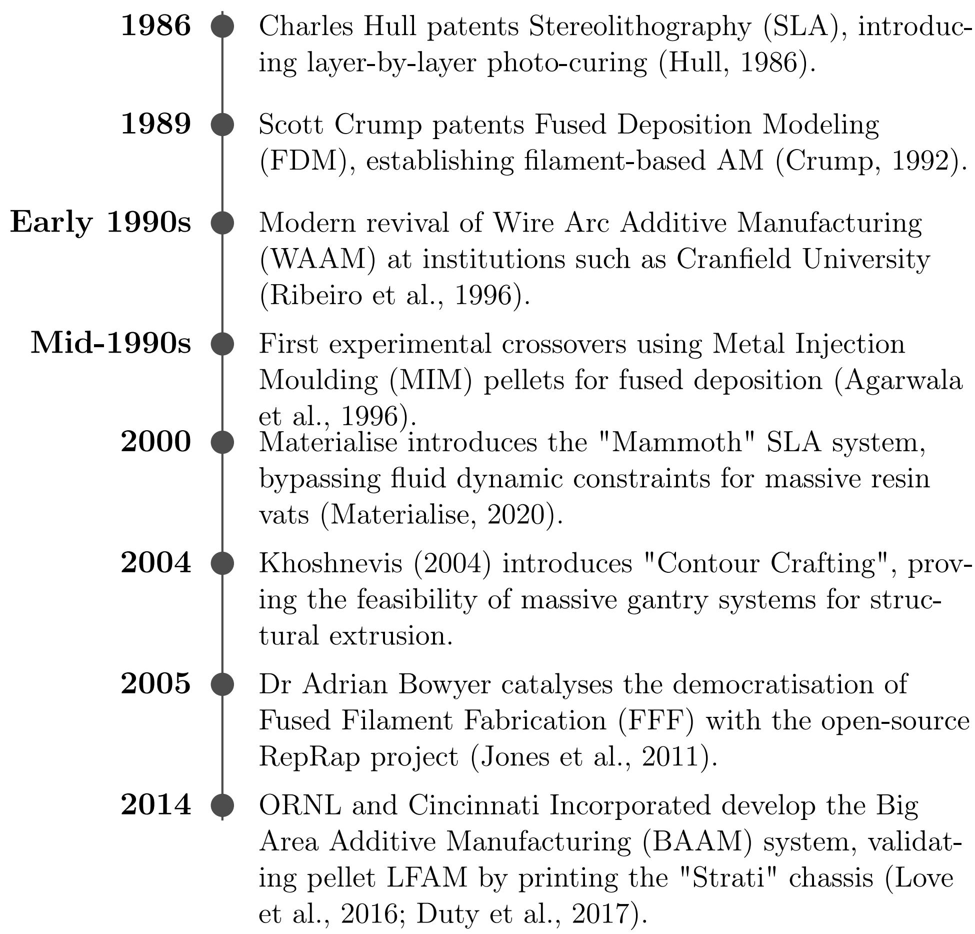

Fig. 1. Timeline of key milestones in the evolution from early Additive Manufacturing to Large-Format Additive Manufacturing.

offshore sector in using metal LFAM for manufacturing parts intended for the marine industry (O'Neill and Mehmanparast, 2024).

Conventional structures are designed to minimise unnecessary movements and ensure that resonance frequencies across different degrees of freedom remain distant from excitation frequencies. In contrast, MRE structures — such as floating WECs — may require enhanced motions to maximise energy capture efficiency (Parmeggiani et al., 2011; Orszaghova et al., 2016; Giannini et al., 2020b,a; Sirigu et al., 2020a; Giannini et al., 2021a; Zanuttigh et al., 2026). These aspects are critical in design, as they may lead to load intensities exceeding conventional model predictions, potentially compromising structural integrity and operational safety. Therefore, these additional requirements can further increase peak wave loads and intensify structure and components fatigue.

Furthermore, MRE devices in order to be economically viable must endure cyclic hydrodynamic loads while minimising structural mass and maintaining long-term functionality. They often integrate internal critical components for buoyancy, stability (e.g., ballasts Ramsay et al., 2022) or power conversion (e.g., power take-off systems Giannini et al., 2020b; Okushemiya et al., 2026), which introduce additional fabrication and technical challenges.

Wave Energy Converters (WECs), Tidal Energy Devices (TEDs), and small vessels — typically ranging from 5 to 30 m in length — may be suitable for manufacturing using plastic materials, including, both thermosets and thermoplastics. For illustration, in Figs. 3 and 4 are shown the main WEC and TED concepts with information of their usual characteristic length (usually the longest dimension) and suitable installation depth, respectively. As these devices have limited dimensions compared to conventional oil and gas structures, their components such as hulls or structural elements could potentially be fabricated using LFAM. However, accurate assessments of external critical loads — particularly those induced by waves, currents, and wind — are essential during the design and material selection.

Figs. 5 to 7 illustrate representative loads acting on these types of structures, i.e. WECs, TEDs and small vessels, respectively. Both high-cycle fatigue loads and extreme load cases must be considered to ensure structural resilience and integrity. For instance, Fig. 5 presents the hydrodynamic loads experienced by an 8.4-metre diameter point absorber WEC, modelled as described by Giannini et al. (2021a, 2025), deployed at a Portuguese offshore site. The design sea states include a typical condition (with a peak wave period T_p = 10 s and a significant wave height H_s = 1.5 m); and extreme (T_p = 16 s; H_s = 11.8 m). In the heave direction, hydrodynamic loads can reach up to approximately 7.4 MN under extreme conditions, while during normal operation they are typically an order of magnitude lower.

For TEDs, rotor-induced bending moments are critical. As shown in Fig. 6, a horizontal-axis turbine with a 20-metre rotor diameter can experience peak bending moments up to 1.25 MN·m (Bir et al., 2011). Under standard operating conditions, these loads are generally less than 40% of the peak values.

In contrast, a 30-metre patrol vessel, as illustrated in Fig. 7, may be subjected to slamming loads that can reach pressures of up to 250 kPa (Muryadin et al., 2023), although during regular operation these loads are typically below 60% of the maximum.

Consequently, the stringent structural requirements and complex loading conditions described above are driving a fundamental evolution in marine design philosophy. Historically, the field relied heavily on manually fabricated GRP structures, which were characterised by limited automation, high labour intensity, and conservative, empirical safety margins. Today, there is a distinct historical shift toward

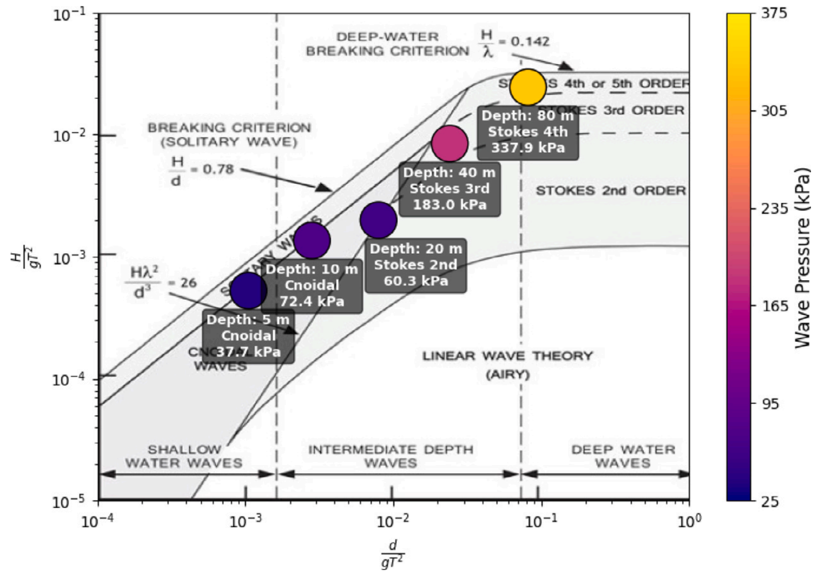

Fig. 2. Wave pressure on a horizontal plate for different type of extreme waves estimated by suitable wave theories, within the Le Méhauté wave diagram.

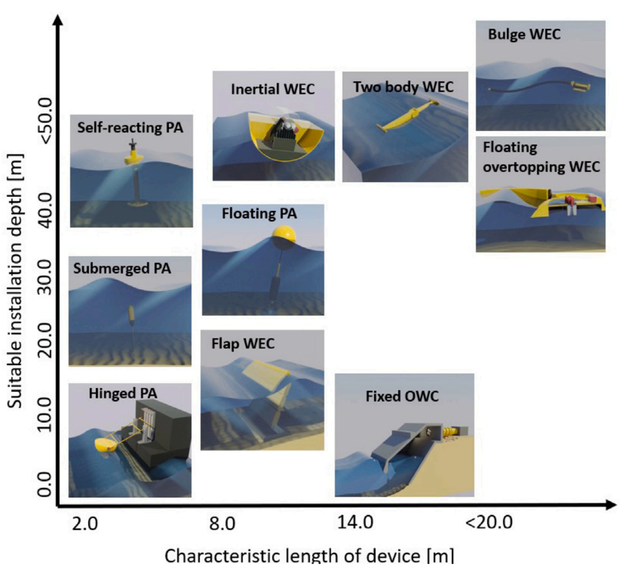

Fig. 3. Main wave energy converter concepts presented by their approximated characteristic length and suitable installation depth.

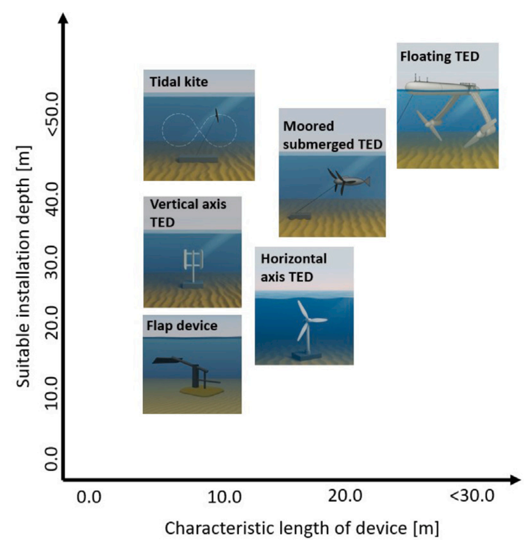

Fig. 4. Main tidal device concepts presented by their approximated characteristic length and suitable installation depth.

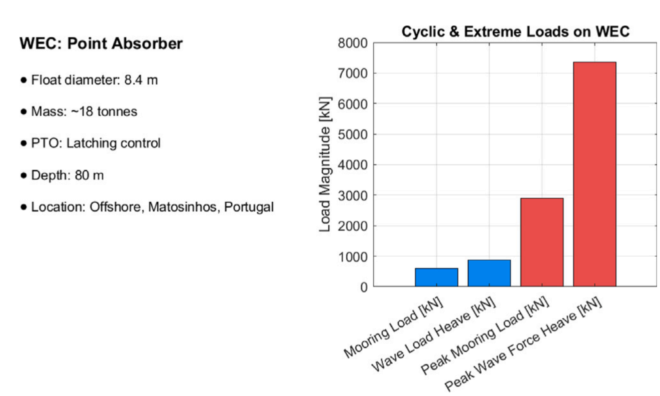

Fig. 5. Example of loads experienced by a wave energy converter.

digitally driven LFAM workflows. This modern paradigm integrates advanced computational simulation, topology optimisation, real-time process monitoring, and data-rich certification pathways, fundamentally transforming how marine structures can be conceived, validated, and manufactured to withstand extreme environments.

3.3. Main challenges for marine fabrication

Marine environments impose stringent requirements on structural integrity, material durability, and fabrication flexibility. In addition to extreme and high cyclic loads, components must withstand saltwater corrosion, biofouling while maintaining performance over extended lifespans (typically up to 20–30 years), with minimal maintenance. These conditions demand not only robust material selection but also careful consideration of joint design, surface treatments, and protective coatings.

Moreover, the large dimensions of offshore platforms and vessels necessitate scalable and modular construction techniques. Traditional

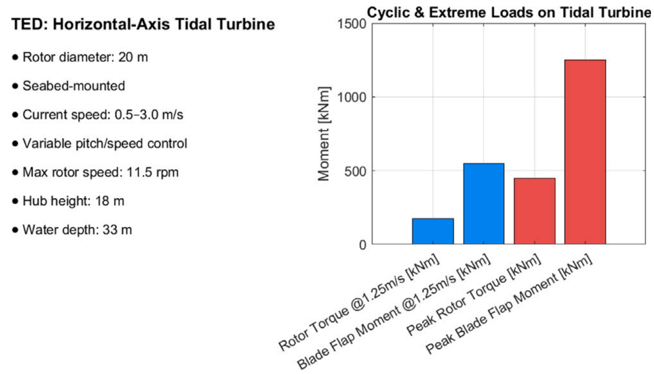

Fig. 6. Example of loads experienced by a tidal energy device.

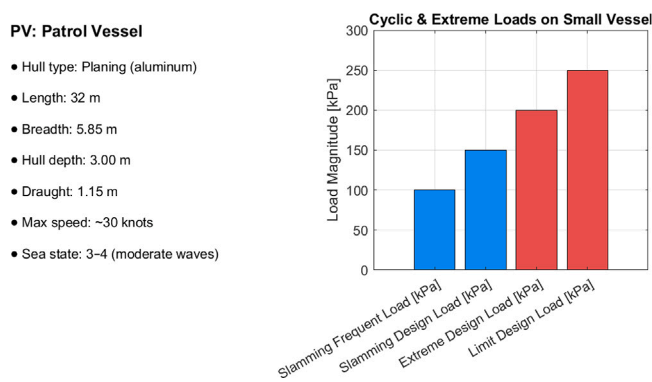

Fig. 7. Example of loads experienced by a patrol vessel.

fabrication methods, such as casting, forging, and composite layup, are often constrained by high labour intensity, long production cycles, and complex logistics, especially when components must be transported and assembled in remote offshore locations. These limitations become even more critical when considering the need for rapid prototyping or on-site customisation, which are increasingly relevant in the context of modular and adaptive marine systems.

Another major aspect is that marine structures must comply with stringent standards set by major classification societies and regulatory bodies, as summarised in Table 2. These standards govern not only structural performance but also material traceability, welding procedures, and inspection protocols. Certifying innovative manufacturing methods — such as additive manufacturing — and novel structural designs remains a significant challenge. This is due to restrictions in material selection, the need for consistent component quality assurance, and the requirement to demonstrate long-term reliability under harsh environmental conditions.

Offshore structures also demand corrosion-resistant materials and geometries optimised for multi-axial loads, often requiring resource-intensive forging or casting (ISO Org., 2020). In this context, the integration of new fabrication technologies must be carefully evaluated against both mechanical performance criteria and regulatory compliance frameworks.

Furthermore, boats and vessels face regulatory constraints concerning buoyancy, fire resistance, and hull integrity (co legislators, 1994).

4. Large-format additive manufacturing overview

LFAM refers to a family of additive manufacturing technologies capable of fabricating components with dimensions exceeding one metre, often using high-output material deposition systems such as pellet extrusion or wire-based directed energy deposition. LFAM systems are engineered to meet industrial-scale production demands by combining rapid deposition rates (often exceeding 10 kg/h), multi-axis robotic control, and compatibility with a wide range of materials, not limited to metals, thermoplastics, concrete and fibre-reinforced options (Huang et al., 2015). The strategic integration of these additive techniques within the marine and offshore sectors is increasingly recognised as a critical enabler for overcoming the severe logistical and supply chain bottlenecks inherent to conventional heavy manufacturing (Veiga et al., 2026).

Large-format polymer systems gained significant traction following the introduction of the first platforms to successfully demonstrate the viability of high-throughput deposition via pellet extrusion. Concurrently, WAAM transitioned from an experimental welding technique to a formalised industrial process, with early large-scale metal demonstrators appearing in the aerospace and civil sectors by the mid-2010s. Additional details regarding the historical milestones of additive manufacturing can be found in the Background section. The transfer of these technologies to the marine sector began in a focused way in the late 2010s and early 2020s. Initial marine applications focused primarily on non-mission-critical components and tooling, such as printed moulds for composite boat hulls. This rapidly progressed to the fabrication of functional prototypes and small craft, notably including the first documented monolithic 3D-printed small vessels and functional WAAM-printed ship propellers (He et al., 2020). This rapid evolution illustrates a transition from generic large-scale prototyping to domain-specific, functional marine manufacturing within a single decade.

Most common AM technologies, printing methods, applicable for producing marine components, are shown in Fig. 8, where also are indicated examples of printable materials. Three main types of technologies can be distinguished, i.e. Extrusion, Photopolymerisation and Powderbed fusion based systems (Tallon and Wilson, 2020). To note that, currently, some of the mentioned technologies, methods and materials appear to not allow producing components larger than 1 cubic metre, therefore they are valid only for small-scale AM.

More specifically, compared to traditional methods, LFAM enables the direct fabrication of large structural components without the need moulds or tooling, reducing material waste and manufacturing time LFAM is increasingly adopted in sectors such as aerospace, construction, and marine engineering (Greer et al., 2019), especially for on-off prints, small productions or moulds making.

LFAM has advanced significantly to meet the complex requirements of the marine sector, particularly in terms of flexibility in printing complex shapes, material adaptability and cost efficiency. Together, thermoplastic LFAM and WAAM, expand the design space for marine applications, supporting the production of simple to articulated geometries, reducing assembly steps through monolithic designs, and offering modular, on-demand fabrication capabilities. Their combined benefits of mechanical performance, reduced tooling needs, and adaptability to hybrid manufacturing systems position LFAM technologies as transformative enablers for the future of marine engineering.

4.1. Robotic architectures and kinematics

To accommodate the dimensions and geometric complexity of marine structures, LFAM relies on a diverse range of kinematic systems, as classified in Fig. 9. These architectures are categorised into three primary classes based on their mobility and axial configuration (Lehmann et al., 2022). In the initial phase of LFAM development, classic small-scale AM architectures, such as Cartesian and later parallel kinematic Delta systems, were simply scaled up to accommodate larger build volumes. Cartesian and Gantry systems remain widely used today for large-format printing, representing a foundational approach that offers

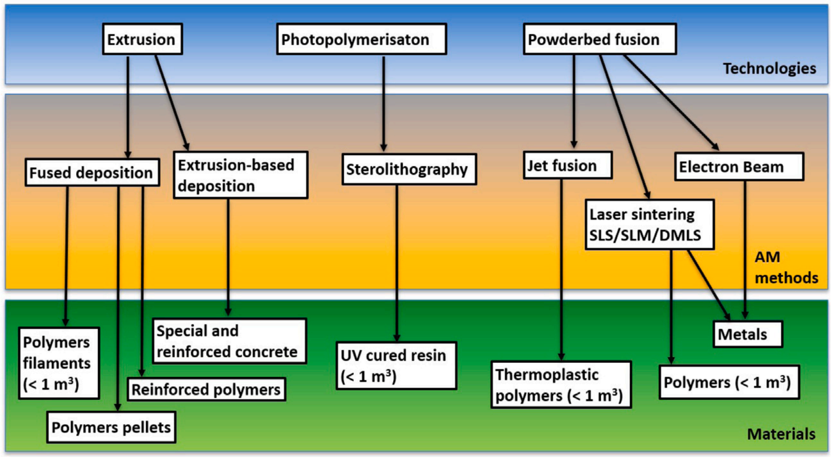

Fig. 8. Main technologies and materials for additive manufacturing.

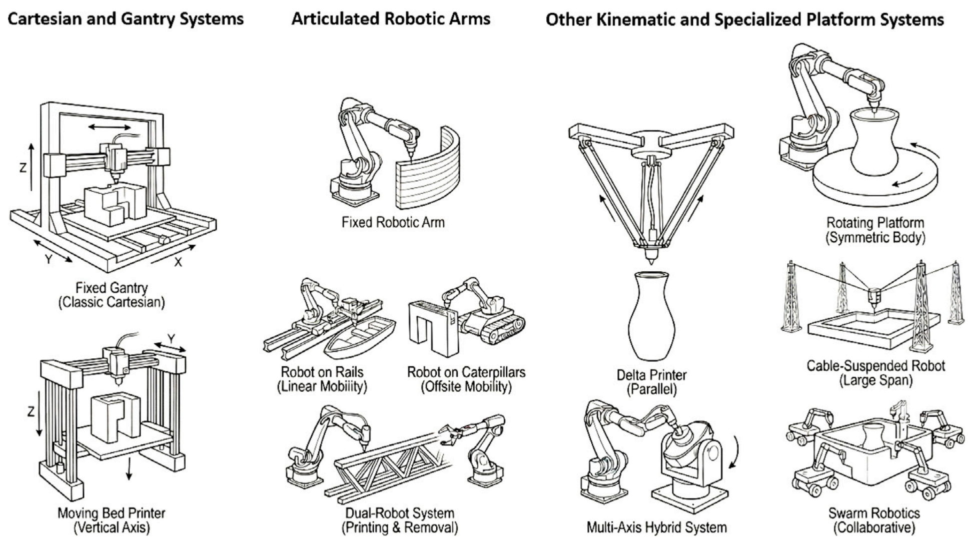

Fig. 9. Taxonomy of Large-Format Additive Manufacturing robotic systems, ranging from standard Cartesian gantries to specialised cooperative and multi-axis configurations for marine applications.

high stability and scalability for massive components, though they are typically limited to 3-axis planar deposition. However, it was found that more specific systems based on articulated robotic arms have been more widely adopted for large-scale printing. These provide up to 6-axis freedom, enabling non-planar printing strategies essential for complex marine geometries (Zhang et al., 2023); crucially, their workspace is frequently extended via metre-scale linear rails or mobile tracked platforms for large-scale on-site, outdoor or mobile fabrication, clearly distinguishing them from conventional small-scale desktop systems (Moreno Nieto and Molina, 2020).

Finally, Specialised and Hybrid Architectures encompass configurations designed for specific geometric or throughput requirements. This includes hybrid solutions integrating robotic arms with rotating build platforms for rotationally symmetric parts. Furthermore, this category includes cooperative multi-robot systems operating strictly at the metre-scale, where synchronised units print simultaneously to reduce lead times, or operate in tandem—with one unit depositing material while another performs subtractive finishing or support removal. This facilitates the fabrication of intricate large-scale structures and directly supports the future mobile and on-site offshore fabrication scenarios envisioned for the marine sector (Zhang et al., 2018; Pignatelli and Percoco, 2022).

4.2. Thermoplastics LFAM

Thermoplastic LFAM systems — particularly pellet-based extrusion — offer promising solutions for polymeric marine structures. These systems can also utilise fibre-reinforced materials such as glass-fibre polypropylene and carbon-fibre reinforced polyamide, which provide high strength-to-weight ratios suitable for buoyant modules, hulls, and deck superstructures. Real-time viscosity and temperature control technologies have improved interlayer adhesion and ensured structural water-tightness, which is a critical parameter in marine environments. Furthermore, thermoplastic LFAM allows rapid and flexible production. For example, in the marine context, complex yacht superstructures up to 8 m long have been printed in under 72 h (Caracol AM, 2026). Similarly, a marine current turbine was developed using AM for the production of a male/internal mould that was successively reinforced by fibreglass, showing high reduction of the manufacturing process time and efforts (Murdy et al., 2021).

Thermoplastic LFAM may well aligns with sustainability goals by enabling the use of recyclable and lower-emission materials. Compared to traditional fibreglass composites, reinforced thermoplastics can reduce carbon emissions to 1/3 compared to traditional methods (Carallo et al., 2025) and offer higher recycling potential (Sola and Trinchi, 2023). These advantages make thermoplastic LFAM an increasingly

Fig. 10. LFAM printed dinghy sailboat made of thermoplastic. Image courtesy of Caracol.

attractive option for the marine sector, especially in applications where corrosion resistance, buoyancy, and performing materials are critical.

As a further example of LFAM for marine applications, in Fig. 10 is shown the thermoplastic LFAM-made Beluga boat. To the best of the authors' knowledge, Beluga represents world's first monolithic 3D-printed dinghy sailboat fabricated using MyReplast — a recycled thermoplastic composite — through an advanced additive manufacturing process developed collaboratively by Caracol and NextChem, a subsidiary of the Maire Tecnimont Group.

4.3. Metal LFAM

Compared to thermoplastic AM, a significantly broader range of metal 3D printing technologies has been proposed and developed. These technologies differ notably in terms of achievable precision, build size, and material compatibility. The main categories include material extrusion (ME), powder bed fusion (PBF), directed energy deposition (DED), material jetting (MJ), binder jetting (BJ), and sheet lamination (SL) (Vafadar et al., 2021).

For LFAM, DED technologies (particularly those based on thermal energy sources) are the most suitable, as they enable the fabrication of high-performance, large-format metal components. Among these, WAAM, a subset of DED, has emerged as a leading approach due to its scalability, material efficiency, and compatibility with standard welding wire feedstock.

WAAM utilises an electric arc to melt metal wire, depositing it layer by layer. Derived from traditional arc welding techniques such as Gas Metal Arc Welding (GMAW), Gas Tungsten Arc Welding (GTAW), and Plasma Arc Welding (PAW), WAAM achieves deposition rates exceeding 10 kg/h. This makes it particularly effective for producing large-scale steel and alloy structures. Its advantages, including low material waste, geometric flexibility, and the use of widely available feedstock, contribute to reduced production costs and shorter lead times. When combined with appropriate materials, these characteristics make WAAM especially well-suited for marine applications, including hull reinforcements, structural frames, and propeller components.

Recent advancements in WAAM include in-situ thermal management and grain refinement strategies, which have significantly improved mechanical consistency. For instance, tensile strengths above 500 MPa have been achieved in low-carbon and duplex steels (Fang et al., 2023). Moreover, hybrid WAAM systems that integrate robotic deposition with subtractive machining have demonstrated up to 40% reductions in post-processing time while enhancing dimensional accuracy (Wu et al., 2018).

A notable marine application of WAAM is the fabrication of ship propellers. As illustrated in Fig. 11, Caracol successfully produced a propeller using WAAM, validating the technology's potential for structurally critical maritime components. This propeller was made using

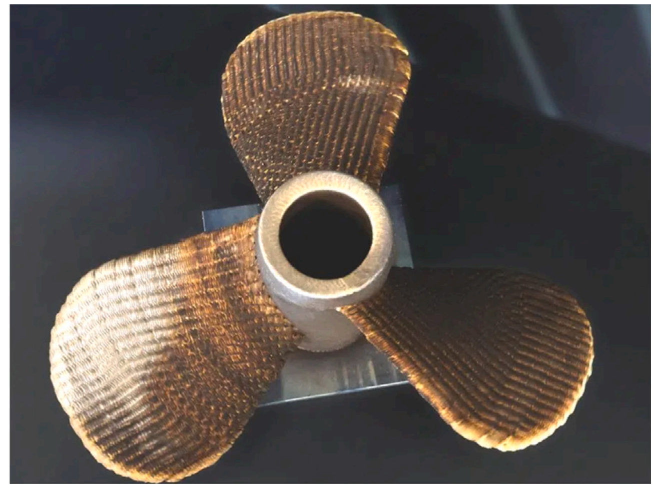

Fig. 11. Example of WAAM-fabricated vessel propeller. Image courtesy of Caracol.

nickel–aluminium bronze (CuAl8Ni6), which is suitable for this type of components because it has superior performance in terms of strength, resistance to corrosion and cavitation. For this sample component of dimensions 750 × 750 × 270 mm and 45 kg of weight, a cold metal transfer type of WAAM was used (Vipra XP proprietary technology) and it took just 10.5 h to print with a deposition rate of 4.6 kg/h. After printing, the propeller had to be post-processed to obtain a smooth surface using a CNC tool.

Demonstrating WAAM's scalability for components exceeding 1 metre is the "WAAMpeller", the world's first class-approved 3D-printed ship propeller (Damen Shipyards Group, 2017). Developed by a consortium including Damen Shipyards Group and RAMLAB, this 1.3-metre diameter, 400 kg propeller was fabricated from corrosion-resistant NAB alloy wire over 298 continuous layers. Following near-net shape deposition, it also underwent extensive CNC milling to meet strict hydrodynamic surface tolerances. Installed on a Damen Stan Tug 1606, it passed rigorous sea trials and received full Bureau Veritas certification, validating WAAM's capability to manufacture massive, highly loaded marine structures that comply with stringent classification society standards.

Beyond WAAM, other thermal energy-based DED processes — such as Laser Metal Deposition (LMD) and Electron Beam Additive Manufacturing (EBAM) — offer additional capabilities. These systems utilise focused energy sources (laser or electron beam) to melt metal powder or wire feedstock, enabling the production of near-net-shape parts with high precision. While these methods typically offer lower deposition rates than WAAM, they provide superior control over microstructure and are increasingly used for high-performance alloys in marine propulsion and repair applications.

Having established the primary kinematic architectures and material deposition technologies (thermoplastics and WAAM), it is imperative to evaluate how these manufacturing methods impact the long-term reliability of the final component.

4.4. Mechanical integrity and fatigue

While the static strength of LFAM components often rivals that of cast or even wrought counterparts, their long-term performance under cyclic marine loads remains a primary subject of industrial validation. The layer-wise deposition inherent to both WAAM and thermoplastic extrusion introduces specific microstructural characteristics — such as porosity, residual stresses, and anisotropy — that distinctively influence fatigue life compared to traditional subtractive manufacturing (Kok et al., 2018). However, recent studies and standardisation efforts demonstrate that when subject to rigorous post-processing and qualification protocols, LFAM components can meet the stringent durability requirements of the marine sector.

While a substantial volume of literature investigates the general mechanical properties of WAAM, the analysis herein focuses on a specific, representative subset of recent studies. These were selected because they explicitly provide quantitative data on high-cycle and low-cycle fatigue limits under pre-corrosion or simulated marine environments, thereby directly addressing the degradation mechanisms relevant to offshore structures.

Research on WAAM indicates that as-built components typically exhibit reduced fatigue life compared to wrought alloys, primarily due to surface roughness acting as stress concentrators and internal defects serving as crack initiation sites. For marine-grade steels and Nickel–Aluminium Bronze (NAB), studies have shown that the "as-built" fatigue limit is significantly compromised by the notch effect of the layer ripples (Shakil et al., 2024). However, this is effectively mitigated through standard post-processing:

- **Surface Finishing:** Machining the surface to remove the outer roughness layer has been proven to restore fatigue performance to levels comparable with cast materials (Pegues et al., 2018).
- **Thermal Treatment:** Post-process heat treatments are essential to relieve the residual thermal stresses induced by the rapid cooling rates of the arc process, further stabilising the microstructure against cyclic crack propagation (Wu et al., 2018).
- **Defect Tolerance:** Fracture mechanics analyses suggest that while gas pores are inevitable, they are generally small enough to be contained within standard safety factors if process parameters are stable. The fatigue behaviour is often dominated by surface defects rather than internal porosity, reinforcing the value of machining critical surfaces (Kasperovich and Hausmann, 2015).

To reflect the latest experimental campaigns, it is essential to consider recent data on both low-cycle and high-cycle fatigue. Recent investigations into the microstructural effects on the high-cycle fatigue properties of WAAM martensitic stainless steel, alongside the influence of pre-corrosion environments on the fatigue response of additively manufactured nickel–aluminium bronze, demonstrate that prolonged exposure to corrosive environments significantly accelerates crack propagation rates compared to in-air testing. However, combining appropriate surface machining with targeted heat treatments has been proven to successfully restore high-cycle fatigue limits to near-wrought levels, even under aggressive marine conditions (Cheng et al., 2023; Roshan et al., 2026).

For polymer composites, the primary fatigue challenge lies principally in the "Z-axis" or inter-layer bond strength. Under cyclic loading, failure frequently occurs via delamination between layers rather than within the filament itself (Sun et al., 2020). In marine environments, this is compounded by the potential for seawater saturation, which can degrade the matrix-fibre interface (Stankovic et al., 2024).

Furthermore, extended seawater immersion studies on fibre-reinforced polymer composites reveal that the degradation of mechanical properties and structural integrity due to hydrothermal seawater ageing severely compromises the inter-layer bond specifically under low-cycle fatigue, underscoring the necessity of marine-specific protective coatings (Yalçınkaya et al., 2025; Alsaadi et al., 2025).

However, design strategies such as alternating layer orientations (e.g., ±45°) and the use of continuous fibre reinforcement have been shown to significantly retard crack growth. Furthermore, manufacturers increasingly apply "knock-down" factors or "derating" coefficients during the design phase, similar to those used for traditional GRP laminates, to conservatively account for long-term property degradation.

The concern regarding fatigue is ultimately an issue of quality assurance rather than a fundamental technology flaw. Major classification societies, including DNV and ABS, have established specific guidelines (e.g., DNV-ST-B203) that shift the focus from generic material properties to "qualified processes" (Junghans et al., 2020). By categorising components based on their criticality (e.g., load-bearing vs. non-structural) and mandating rigorous non-destructive testing (NDT), witness builds, and destructive testing of production coupons, the uncertainty regarding fatigue life is managed (Honarvar and Varvani-Farahani, 2020). Consequently, if an LFAM component is properly designed with appropriate safety factors, post-processed to remove stress raisers, and validated against class society standards, its fatigue performance might be functionally equivalent to certified traditional marine structures.

To properly contextualise the current state of the art, it is essential to balance foundational AM literature with very recent domain-specific developments. Recent comprehensive reviews have meticulously documented the leap in large-format polymer extrusion capabilities (Pignatelli and Percoco, 2022; Goh et al., 2024). Similarly, the understanding of WAAM has rapidly evolved from foundational process overviews (Wu et al., 2018) to cutting-edge analyses of process-structure-properties linkages (Zhang et al., 2024). Furthermore, this technological maturation is now being directly translated into the maritime sector, as highlighted by the latest reviews focusing exclusively on additive manufacturing applications for marine vessels and offshore structures (Peterson, 2022; Belvisi et al., 2024; Sözen and Neşer, 2025).

4.5. Standards and certification landscape

The increasing adoption of LFAM across industrial sectors has underscored the urgent need for comprehensive standards that address design integrity, process qualification, and sustainability. In contrast to small-scale additive manufacturing, LFAM typically involves pellet-fed extrusion of thermoplastics or fibre-reinforced composites at the metre scale. This shift in scale introduces new technical challenges, including variability in feedstock quality, machine calibration and validation, dimensional accuracy over large build volumes, and subsystem-level energy efficiency. These aspects become particularly critical in marine engineering applications, where structural components are exposed to demanding operational environments and must comply with rigorous safety, performance, and durability criteria, e.g. Gonzales and Kujala (2021).

In this context, the role of international standards is pivotal. As summarised in Table 2, existing frameworks from ISO/ASTM and SAE provide structured guidance across multiple domains, including design optimisation, quality assurance, process validation, data interoperability, and environmental management. Although many of these standards were originally developed for metal powder bed fusion or small-scale extrusion systems, their underlying principles — such as traceability, repeatability, and process control — are also applicable to LFAM. Moreover, several standards are currently being revised or extended to explicitly accommodate polymer-based LFAM and composite processes.

For marine applications, LFAM offers promising opportunities in the fabrication of lightweight yet robust components, such as hull segments, tooling structures, and outfitting elements. In these cases, adherence to established standards is not only beneficial but essential. It ensures that printed parts meet certification requirements, facilitates reproducibility across manufacturing sites, and supports long-term integration of LFAM technologies into regulated maritime and naval sectors.

Beyond generic ISO/ASTM standards, major marine classification societies have recently introduced dedicated guidelines specifically tailored to the qualification of AM processes and parts for the marine, offshore and energy domain. For instance, DNV has continuously updated its DNV-ST-B203 standard, which now provides a comprehensive framework for both metallic and polymer AM parts, including specific metrics for carbon footprint and guidance on part-family qualification. Similarly, the American Bureau of Shipping (ABS) has published its Requirements for Additive Manufacturing, detailing standardised processes for qualifying 3D-printed materials, equipment, facilities and parts for marine and offshore applications. Furthermore, Lloyd's Register (LR) has recently released updated Guidance Notes for the Manufacture, Testing, and Certification of Additive Manufactured Metallic Parts and separate Guidance Notes for Polymer Additive Manufacturing Certification, shifting from a generic industrial approach to one focused on marine and offshore service. These frameworks are pivotal for transitioning LFAM from prototyping to the deployment of mission-critical, class-approved marine assets.

4.6. Fit of LFAM to marine requirements and added features

Given the harsh operational conditions earlier described, materials and manufacturing approaches must ensure both mechanical durability, particularly fatigue resistance, and corrosion resistance over extended service time-frames.

Especially for MRE installations, sustainability and circular economy goals are increasingly influencing marine engineering. This has spurred interest in recyclable thermoplastics such as polypropylene (PP), high-density polypropylene (HDPP), and polyethylene terephthalate glycol (PETG), which are compatible with LFAM. Compared to classic GRP, thermoplastic-based LFAM components can reduce lifecycle carbon emissions by up to 22% (Caracol AM, 2026). Economically, LFAM enables cost savings through near-net-shape manufacturing, reducing both raw material waste and post-processing requirements. For example, hybrid WAAM-machining systems have demonstrated component cost reductions of approximately 72% (Feier et al., 2023).

4.7. Additional features of LFAM for marine applications

LFAM offers significant advantages for marine manufacturing. On-site or near-site fabrication reduces transportation costs and enables just-in-time production, especially critical for offshore deployment. The ability to fabricate complex geometries through digital workflows allows for topology optimisation, integrated functionality, and material-efficient designs. Therefore if LFAM is applicable, this can eliminates the need for large moulds or dies, shortening lead times and lowering initial tooling investments. These benefits are particularly valuable for custom or low-volume marine components, pilot devices of limited sizes, marine turbine blades, buoyancy modules, and geometric articulated components. To facilitate the selection of the most appropriate method for these applications, Table 3 provides a brief summary of the two primary LFAM technologies — Thermoplastic extrusion and Metal WAAM — highlighting their distinct feedstocks, deposition capabilities, and specific advantages for the marine sector.

4.8. Roadmap and evolution of marine LFAM applications

The current implementation of LFAM in the marine sector follows an evolutionary pattern of application. Initially, adoption focussed on tooling, moulds, and non-critical secondary parts, where the primary goal was reducing manufacturing lead times without the need to confront stringent structural certification. As the technology matured, applications progressed to functional prototypes and complete small craft. Additional, notable case studies in this domain include the 3Dirigo, a 25-foot vessel produced by the University of Maine in 2019, which holds the record as the largest 3D-printed boat fabricated in a single operation using carbon fibre-reinforced thermoplastic. Similarly, the MAMBO (Motor Additive Manufacturing Boat), launched in 2020 by Moi Composites, demonstrated the feasibility of continuous fibre-reinforced composites for complex, wave-inspired hull geometries. Further commercial implementations are exemplified by thermoplastic-printed vessels like the Beluga, as well as production runs by companies such as Tanaruz and CEAD (CEAD Group, 2024), which utilise recycled polymers to prioritise circular economy principles in small boat manufacturing (Ziółkowski and Dyl, 2020).

Currently, the industrial frontier has advanced to mission-critical, highly loaded components that demand rigorous certification. A landmark achievement in this area was the fabrication of the world's first class-approved WAAM marine propeller by Damen Shipyards Group and RAMLAB in 2017, a 1300 mm diameter, 180 kg bronze component certified by Bureau Veritas (He et al., 2020; Lampros and Zervaki, 2026). The offshore sector has also accelerated this transition; for instance, Vallourec and TotalEnergies recently deployed the first WAAM-produced pressure-containing waterbushing and load-carrying lifting plugs (capable of bearing 100 metric tonnes) in the North Sea, validating the technology for safety-critical marine operations (Caron et al., 2025).

Extrapolating this trajectory into a forward-looking roadmap, near-term developments will likely focus on increasing the TRL for marine demonstrators and accumulating robust, well-documented case studies. In the mid-term, the sector anticipates the first class-approved primary LFAM structures and the consolidation of standardised certification workflows. Ultimately, the long-term scenario envisions widespread industrial adoption, where full primary load-bearing structures — such as MRE floaters — and complex multi-material modules are routinely printed and seamlessly integrated with multi-use offshore platforms (Choi et al., 2024).

5. Innovative 3D-printable materials

Research on suitable and new materials is crucial for the adoption of LFAM in the marine sector. Innovations include recyclable thermoplastics, corrosion-resistant metals, and fibre-reinforced hybrid solutions tailored for underwater or load-bearing applications. Circular material strategies, such as using recycled polymers or biodegradable binders, contribute to sustainability goals and reduce life-cycle environmental impact. The selection of suitable LFAM materials must consider not only mechanical and environmental performance but also cost, printability, and regulatory compliance. Given the scope of this study, only some examples of feasible materials for marine use are provided in this section.

5.1. Polymers materials

The preparation of plastics for additive manufacturing (AM) involves a multi-level industrial supply chain, each stage contributing to the transformation of raw chemical inputs into high-performance materials suitable for 3D printing, Fig. 12. This process can be structured into four distinct levels:

- **Level 1—Monomers:** The supply chain begins with monomers, which are the fundamental chemical building blocks. These are typically in liquid or gaseous form and undergo polymerisation reactions to form long-chain macromolecules known as polymers.
- **Level 2—Polymers:** The resulting polymers are usually processed into pellet form. At this stage, materials are chemically stable but might lack the specific mechanical, thermal, or rheological properties required for AM applications.
- **Level 3—Compounded Polymers:** Polymers are then compounded with additives, fillers, reinforcements, or other polymers to tailor their properties. This compounding process results in customised polymer blends, still in pellet form, optimised for specific AM technologies or performance requirements.
- **Level 4 (optional)—Filaments:** Finally, the compounded pellets are extruded into filaments through a controlled thermal and mechanical process. These filaments are the final feedstock used in filament-based additive manufacturing processes, such as Fused Filament Fabrication (FFF).

Table 2
Standards and guidelines relevant to Large-Format Additive Manufacturing.

Standard (Date)	Name	Relevance to LFAM
ISO/ASTM 52910:18	Design—Requirements, guidelines	AM design rules for robust LFAM geometry and reduced waste.
ISO/ASTM 52901:17	General principles—Purchased AM parts	Procurement criteria and traceability for LFAM part qualification.
ISO/ASTM 52920:23	Qualification principles—Ind. AM processes	Site-level qualification: process control, personnel, equipment.
AMS7011 (SAE), 22	EB-PBF Preforms—Ti-6Al-4V—HIP	Aerospace spec; reference for high-criticality AM qualification.
ARP7042 (SAE)	Design of AM Components in Aircraft	Certification planning and risk flow-down for LFAM in aerospace.
Material extrusion (polymer) and LFAM-focused		
ISO/ASTM 52903-1:20	Mat. extrusion—Part 1: Feedstock	Feedstock specs for pellet-fed LFAM: moisture, size, melt flow.
ISO/ASTM 52903-2:20	Mat. extrusion—Part 2: Equipment	Hardware/process requirements for LFAM setup and acceptance.
ASTM F3529-21	Guide—Design—Mat. Extrusion (Poly)	Design guidance for LFAM: bead size, raster, overhangs.
ASTM F3489-23	Guide—Mat. handling & static prop.	Best practices for LFAM polymer testing and reporting.
Validation, capability, data and reporting		
ISO/ASTM 52902:19	Test artefacts—Geometric capability	Accuracy/distortion mapping for LFAM build volumes.
ISO 17295:2023	AM—Part positioning, coordinates	Coordinate/orientation rules for LFAM and machining.
ISO/ASTM 52950:21	Overview of data processing	AM data chain for LFAM job tickets and traceability.
ISO/ASTM 52915:20	Additive Manufacturing File Format (AMF)	Rich geometry/metadata format for LFAM builds.
ASTM F2971-13(21)	Reporting Data for AM Test Specimens	Harmonised reporting for LFAM material datasets.
ISO/ASTM 52900:21	Fundamentals and vocabulary	Controlled terminology for LFAM documentation.
EHS and energy management		
UL 2904	Particle/chemical emissions	Emissions limits for LFAM enclosures and ventilation.
ISO 50001:2018	Energy management systems	Framework to improve LFAM cell energy performance.
Marine Classification Society Guidelines		
DNV–ST–B203	Additive manufacturing	Qual. framework for AM *metals and polymer* for energy & maritime; includes CO_2 appendix (Nov 2025 ed.).
ABS 322	Requirements for Additive Manufacturing (July 2022)	Standardised qualification of AM facilities, feedstock & parts for *marine and offshore*.
LR Guidance Notes (Metallic)	Guidance Notes: AM Metallic Parts (Jun 2024)	Goal-based certification to meet class requirements for *ships and offshore*.
LR Guidance Notes (Polymer)	Guidance Notes: Polymer AM Certification (Apr 2024; update Jul 2025)	Goal-based certification for polymer AM parts in *marine and offshore* service.

Table 3
Comparison of key features between Thermoplastic LFAM and Metal LFAM (WAAM) for marine applications.

Feature	Thermoplastic LFAM (Pellet extrusion)	Metal LFAM (WAAM)
Primary Technology	Material Extrusion (FGF/BAAM)	Directed Energy Deposition (DED-Arc)
Feedstock State	Thermoplastic pellets (often fibre-reinforced)	Standard welding wire (Steel, Al, Ti, NAB)
Deposition Rate	High (typically 10–50 kg/h depending on nozzle)	High (> 10 kg/h for steel/Al alloys)
Marine Advantages	Corrosion immunity, high specific strength (buoyancy), recyclability.	High structural integrity, ductility, isotropic potential, repair capability.
Key Limitations	Anisotropy (Z-strength), UV degradation (needs coating), lower thermal limit.	High thermal stresses (distortion), significant post-process machining required.
Typical Applications	Hulls (small vessels), superstructures, moulds/tooling, buoys.	Propellers, structural joints, ribs, heavy-duty repair/spare parts.
Post-Processing	Surface smoothing, coating/painting, minimal machining.	Stress relieving (heat treatment), CNC machining for tolerances.
Cost Drivers	Material cost (specialty pellets), machine volume.	Energy consumption, post-processing (machining) time.

As materials progress through each level of the supply chain, additional processing steps — such as polymerisation, compounding, and extrusion — introduce increasing levels of complexity, energy consumption, and quality control. Consequently, the cost of the material increases significantly at higher levels, particularly at Level 4, where the material is fully processed and ready for direct use in usual small-scale 3D printers.

Standard 3D printers normally use polymers in filament form (1.75 mm/ 2.85 mm diameter) for producing parts via a fused filament fabrication (FFF) process. FFF is compatible only for suitable polymers having adequate material properties that allow a reliable extrusion. Filaments are created in advance and can be found on the market in various blends, typically priced at over ten times the cost of the original raw materials (pellet form). The quality of the filament influences considerably the success of 3D prints. The larger the object being printed, the greater the risk of failure. Therefore, usually, filaments are used for producing small components, normally not exceeding 1 m^3. Usual FFF filaments are PLA (Polylactic Acid), ABS (Acrylonitrile

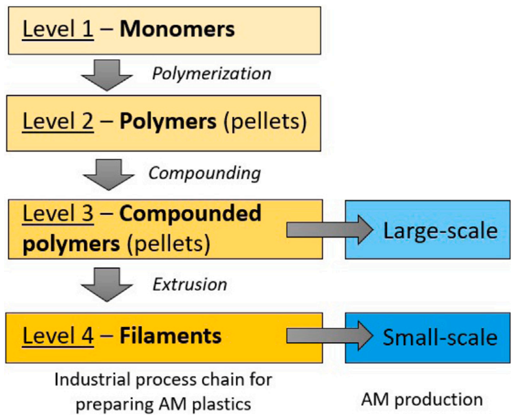

Fig. 12. Levels of the industrial supply chain for additive manufacturing plastic preparation.

Butadiene Styrene), Nylon and reinforced variances. Although several plastic materials options exist, ranging from flexible, high-performance materials to transparent.

Mainly for large-scale components, pellet systems appear to be much more suitable because do not require the filament preparation process (Kumar et al., 2022). Polymer pellets are small, typically spherical or barrel-shaped granules a few millimetres in diameter, available as raw materials in the plastic marketplace. Common types include ABS, PP (Polypropylene), HDPE (High-Density Polyethylene), LDPE (Low-Density Polyethylene), PVC (Polyvinyl Chloride), and PET (Polyethylene Terephthalate). Plastics, defined as organic high polymers that retain shape after force is removed, are broadly categorised into thermoplastics, elastomers, and thermosets.

Thermoplastics, which can be repeatedly melted and reshaped without significant chemical degradation, are further divided into semicrystalline and amorphous types. Semicrystalline polymers, with 10%–80% crystallinity, have ordered molecular structures and distinct melting points, while amorphous polymers have irregular molecular arrangements and transition from rigid to rubbery states at their glass transition temperature.

Thermoplastics are also classified by application into commodity, engineering, and high-performance plastics. Commodity plastics, such as PE (Polyethylene), PVC (Polyvinyl Chloride), PP (Polypropylene), and PS (Polystyrene), are produced in large volumes for everyday use and are cost-effective but have lower mechanical properties. PE (Polyethylene), the most widely used, is versatile and can be tailored in density and crystallinity to suit various applications, with HDPE (High-Density Polyethylene) offering strength and LDPE (Low-Density Polyethylene) providing chemical resistance.

Examples of typical LFAM materials used for marine applications are summarised in Table 4. From the broader pool of identified literature concerning polymer feedstocks for additive manufacturing, these specific examples were selected because they provide explicit, comparative data on critical marine parameters — such as mechanical strength, water absorption, and chemical resistance — ensuring a representative rather than arbitrary cross-section of available commodity and engineering plastics. HDPE is a low-cost, chemically resistant polymer with excellent water resistance and recyclability, making it suitable for buoyant or less structural-critical marine components. However, its poor UV resistance and low mechanical strength limit its use in exposed or load-bearing applications, e.g. Peterson (2022). PP is another promising candidate, offering a lightweight, corrosion-resistant, and cost-effective solution for marine use, e.g. Volpato et al. (2015), Moreno Nieto et al. (2018). Nylon 12 can be used for LFAM and provides excellent strength and durability, though its high cost and water absorption limit its broader application, e.g. Garofalo et al. (2024). ABS is widely used for prototyping due to its printability and moderate strength, but it suffers from poor UV resistance, e.g. Murdy et al. (2021). TPU, while flexible and impact-resistant, is not suitable for structural parts, although it is envisioned that may be relevant for specific use, for instance to make fenders for marine use, e.g. Pinho and Piedade (2025). PLA is biodegradable and easy to print, but its poor durability in outdoor environments restricts its use if not well coated, e.g. Belvisi et al. (2024). PETG offers a good balance of strength, chemical resistance, and recyclability, making it a strong candidate for LFAM in marine settings. However, its relatively low glass transition temperature ($T_g \approx$ 80°C) poses a risk of thermal deformation; specifically, dark-coloured components may soften due to heat accumulation under high solar irradiance (Nieto and Molina, 2020), necessitating the use of reflective coatings or light pigmentation.

On the market already exist high-performing AM materials in the form of pellets that can be suitable for marine use. For instance, SABIC's portfolio of AM compounds for pellet-fed AM (Sabic, 2022) includes high-performance thermoplastics such as ABS, PPE (Polyphenylene Ether), PC (Polycarbonate), PEI (Polyetherimide), PC/PBT (Polycarbonate/Polybutylene Terephthalate blend), PESU (Polyethersulfone), each reinforced with carbon or glass fibres to enhance mechanical properties, Fig. 13. For marine applications, materials with low water absorption, high dimensional stability, and resistance to hydrolysis are critical. PPE-based compounds offer excellent moisture stability and low thermal expansion, making them well-suited for marine environments (Pros: hydrolytic stability, dimensional stability; Cons: lower strength than PC, limited high-heat resistance). PEI-based compounds, provide superior strength-to-weight ratio and thermal resistance (Pros: high temperature performance, low creep; Cons: higher cost, more complex processing). PC/PBT blends offer improved chemical resistance and low warpage (Pros: chemical resistance, processability; Cons: moderate thermal performance, potential UV sensitivity). While ABS and PC compounds are easier to process and cost-effective, their lower resistance to moisture and thermal cycling may be less performing for some marine applications.

5.1.1. Circularity and recycled pellet case studies

In addition to virgin and specific compounds, the transition towards a circular economy in the maritime sector is driving significant advancements in recycled thermoplastic feedstocks for large-format printing (Murdy et al., 2024). This transition is increasingly supported by industrial case studies demonstrating the viability of closed-loop material life cycles. The process typically involves upcycling industrial scrap and end-of-life materials by shredding them into small, uniform flakes, which are subsequently repelletised and re-extruded as feedstock for new large-format prints. Integrating these recycling processes directly into the LFAM workflow allows for the production of functional, large-format components without severe degradation in mechanical properties, thereby drastically reducing the environmental footprint and material costs associated with massive marine prototyping and structural production (Bas-Bolufer et al., 2025; Korey et al., 2025).

Recent implementations highlight the feasibility of this approach across various industrial sectors:

- **Composite Tooling and Moulds:** Industrial collaborations have demonstrated that thermoplastic composite trimming fixtures and moulds can be efficiently recycled after their service life. Large-format moulds are processed through single-shaft shredders into uniform flakes (typically around 10 mm) and directly re-processed in LFAM systems to manufacture new tooling, significantly reducing dependency on virgin materials and lowering logistics costs (CEAD Group, 2024).
- **Construction Formworks:** In the civil engineering sector, large-format 3D-printed polymer composite formworks used for casting precast concrete have been successfully recycled. Studies show that after high-pressure washing to remove cementitious

Table 4
Example of thermoplastic materials used for marine applications, their properties and suitability of LFAM. Symbols: ρ = density, σ_t = tensile strength, E = Young's modulus, T_t = thermal transition, W_{abs} = water absorption. Abbreviations: Chem. = chemical resistance, Mod. = moderate, Recycl. = recyclability, Print. = printability score for LFAM.

Material	ρ (g/cm^3)	σ_t (MPa)	E (GPa)	T_t (° C)	Chem.	UV	W_{abs} (%)	Recycl.	Cost (€/kg)	Print.	Ref.
HDPE	0.95	20	0.8	130 (Tm)	High	Poor	0.01	High	1.5	High	Peterson (2022)
PP	0.90	30	1.5	160 (Tm)	Good	Mod.	0.01	High	1.8	High	Moreno Nieto et al. (2018)
Nylon 12	1.02	75	1.7	178 (Tm)	High	Mod.	1.4	Low	15	Mid	Garofalo et al. (2024)
ABS	1.04	40	2.1	105 (Tg)	Mod.	Poor	1.0	Med.	2	High	Murdy et al. (2021)
TPU	1.20	45	0.05	180–220 (Tm)	Mod.	Mod.	1.2	Low	3	Mid	Pinho and Piedade (2025)
PLA	1.24	60	3.5	150–180 (Tm)	Low	Poor	0.5	High	2	High	Belvisi et al. (2024)
PETG	1.27	50	2.0	85 (Tg)	Good	Mod.	0.2	High	2.5	High	Moreno Nieto et al. (2021)
PPS	1.35	90	3.5	280 (Tm)	Excell.	Good	0.02	Low	12	High	Roseman et al. (2016)
POM	1.41	70	3.0	165 (Tm)	Good	Poor	0.25	Medium	2.5	Low	Roseman et al. (2016)
PVDF	1.78	40	2.0	170 (Tm)	Excell.	Good	0.04	Medium	8	Mid	Roseman et al. (2016)

Name	Description	σ_{t-x} (MPa)	σ_{t-z} (MPa)	σ_{f-x} (MPa)	σ_{f-z} (MPa)
PEI-20CF EM	Polyetherimide (Easy Molding), 20% Carbon Fiber	158.88	54.32	217.58	69.51
PEI-20CF	Polyetherimide, 20% Carbon Fiber	132.89	47.61	188.67	65.71
PC-20CF	Polycarbonate, 20% Carbon Fiber	123.54	48.48	164.43	66.30
PC/PBT-20CF	Polycarbonate/Polybutylene Terephthalate, 20% Carbon Fiber	105.43	27.16	149.24	38.84
FR PC-20CF	Flame Retardant Polycarbonate, 20% Carbon Fiber	104.26	37.38	136.97	52.86
PEI-20GF	Polyetherimide, 20% Glass Fiber	94.04	39.14	137.56	61.92
ABS-20CF	Acrylonitrile Butadiene Styrene, 20% Carbon Fiber	89.08	17.52	125.29	32.71
PC-20GF	Polycarbonate, 20% Glass Fiber	87.32	44.39	138.73	64.54
High heat PC-20CF	High Heat Polycarbonate, 20% Carbon Fiber	86.45	19.57	108.64	28.33
PEI-30mGF	Polyetherimide, 30% Mineral Glass Fiber	83.53	45.27	131.43	67.46
PESU-20CF	Polyethersulfone, 20% Carbon Fibe	82.65	24.82	105.14	37.38
PPE-20CF	Polyphenylene Ether, 20% Carbon Fiber	74.47	21.32	99.01	35.92
PPE-20GF	Polyphenylene Ether, 20% Glass Fiber	68.34	27.75	103.39	51.11
ABS-20GF	Acrylonitrile Butadiene Styrene, 20% Glass Fiber	61.62	21.61	91.12	34.46

Fig. 13. Example of high-performing thermoplastics compounds for LFAM. Brighter colours indicate higher values. Based on data provided by Sabic (2022).

contamination, the thermomechanical recycling of these formworks allows the material to be reused for printing new formworks. While minor reductions in fibre length and material viscosity occur, thermal stability and functional effectiveness are maintained (Schweizer et al., 2024).

- **Wind Turbine Blade Upcycling:** Addressing the massive waste generated by decommissioned wind turbine blades, recent research initiatives have successfully coupled repurposing methods with LFAM. By shredding decommissioned glass and carbon fibre-reinforced plastics (GFRP/CFRP) and compounding them with a polymer matrix, the recovered fibres serve as reinforcement in new LFAM pellets. These recycled pellets have been subsequently used to 3D print large structural elements (Henao et al., 2023).

These cross-sectoral case studies validate that integrating shredding and repelletising processes directly into the LFAM workflow is not only technically viable but essential for achieving scalable, sustainable manufacturing in heavy industries, including the marine sector.

5.2. Metals

While a wide variety of metals can be processed using AM, only a subset is suitable for the demanding conditions of marine environments. The selection of metals for LFAM in marine applications is primarily guided by their corrosion resistance, mechanical strength, and long-term durability.

Metals commonly considered for LFAM in marine contexts include:

- **Stainless steels:** particularly austenitic and duplex grades, known for their corrosion resistance and mechanical reliability.
- **Copper-nickel alloys:** offer excellent resistance to seawater corrosion and biofouling, making them suitable for piping systems and heat exchangers.
- **Titanium alloys:** valued for their high strength-to-weight ratio and exceptional corrosion resistance, especially in deep-sea applications.
- **Aluminium alloys:** lightweight and corrosion-resistant, often used in superstructures and lightweight marine components.
- **Nickel-based superalloys:** provide superior mechanical performance and corrosion resistance in extreme environments.

Among the most interesting applications there is nickel–aluminium bronze (NAB), a material widely used in the maritime industry for components such as ship propellers and pump housings. NAB offers excellent resistance to corrosion and cavitation, making it ideal for both manufacturing and repair of critical parts. Notably, recent advancements have demonstrated the feasibility of printing NAB even in underwater conditions, expanding its potential for in-situ repairs (Keshavarzan and Mohammadi, 2024).

Furthermore, conventional structural steels such as S355 are being investigated as a baseline for developing new alloys with improved corrosion resistance and AM compatibility (Ibrahim et al., 2024).

Beyond NAB and baseline structural steels, recent research has increasingly focused on advanced marine-grade corrosion-resistant alloys for WAAM, specifically targeting highly demanding offshore and ship components. Duplex and Super Duplex stainless steels (such as ER 2209) have been successfully evaluated and processed via WAAM to manufacture critical pressure-retaining components and automotive/marine systems that must withstand aggressive, high-temperature marine environments. The rigorous evaluation of their mechanical and metallurgical properties, alongside the optimisation of heat treatment temperatures, has proven essential in controlling phase composition, enhancing mechanical strength, and maximising corrosion resistance to meet stringent maritime operational standards (Aravind et al., 2025; Karunanithi et al., 2026).

In addition to more established materials, research is actively exploring advanced alloys and composites tailored for marine LFAM. These include functionally graded materials, which allow gradual transitions in composition or structure to optimise performance; nanostructured metals, which enhance strength and corrosion resistance; and corrosion-resistant metal matrix composites (Vafadar et al., 2021).

6. Surface roughness and drag effect

As established in Section 3 regarding severe hydrodynamic loads and in Section 4 concerning the inherent "staircase" deposition of LFAM technologies, managing the structural-fluid interface is a primary engineering challenge. One of the most distinct characteristics of components produced via LFAM is the surface finish. Unlike the smooth surfaces typical of moulded composite or steel-made parts, LFAM components exhibit a periodic, corrugated surface texture resulting from the layer-by-layer deposition process. This "stair-stepping" effect is governed by the layer height (L_h), which in pellet-based extrusion typically ranges from 0.5 mm to over 5.0 mm. In the context of marine hydrodynamics, this surface roughness (k_s) can significantly alter the boundary layer flow, leading to potential increases in skin friction drag (Volino et al., 2011; Flack and Schultz, 2014). It must be explicitly noted that the analytical expressions presented herein are established, deterministic engineering parameterisations used for preliminary assessment, and do not constitute novel statistical modelling or data fitting derived from this review. Understanding the hydrodynamic penalty of LFAM roughness requires analysing the flow regimes governed by the Reynolds number (Re), defined as:

$$Re = \frac{U\,L}{\nu} \tag{1}$$

where U is the flow velocity, L is the characteristic length of the structure, and ν is the kinematic viscosity of seawater ($\approx 1.19 \times 10^{-6}$ m^2/s).

To estimate the drag penalty, the skin friction coefficient (C_f) is estimated by combining theoretical baselines for smooth and rough turbulent flows. The smooth flow regime is governed by the ITTC-57 model-ship correlation line (White, 2016; Zeng et al., 2019; Wrzask, 2023):

$$C_{f,smooth} = \frac{0.075}{(\log_{10} Re - 2)^2} \tag{2}$$

For the rough regime, the maximum possible friction is calculated using Schlichting's formula for rough flat plates. This formula provides a constant friction value that depends only on the characteristic length (L) and the roughness height (k_s) (White, 2016):

$$C_{f,rough} = \left(1.89 + 1.62 \cdot \log_{10}\left(\frac{L}{k_s}\right)\right)^{-2.5} \tag{3}$$

The final friction curve can be estimated by taking the maximum of these two values, $C_f = \max(C_{f,smooth}, C_{f,rough})$. This simple approach captures the transition where roughness elements protrude through the viscous sublayer, causing the flow to shift from a smooth behaviour to a fully rough behaviour.

6.1. Implications for different marine cases and mitigation strategies

The impact of LFAM-induced surface roughness on hydrodynamic performance varies significantly depending on the specific operational flow regime of the marine structure. Fig. 14 illustrates the relationship between Reynolds number and skin friction coefficient for a structure with length $L = 10$ m, assuming a standard seawater kinematic viscosity of $\nu \approx 1.19 \times 10^{-6}$ m^2/s, thereby highlighting the deterministic nature of these visualised engineering bounds. The plot compares the smooth friction line (ITTC-57 correlation) against the friction caused by LFAM surfaces with roughness values of $k_s = 0.5, 1.0, 2.0,$ and 4.0 mm. As shown in the graph, at lower Reynolds numbers, the curves follow the smooth line because the roughness is effectively submerged in the boundary layer. However, as Re increases, the curves separate from the smooth line and levelling off at a constant, higher value.

Such analysis highlights three distinct, overlapping operational zones for marine devices:

- **Wave Energy Converters (WECs):** Characterised by oscillatory motions and moderate flow velocities, WECs typically operate at Reynolds numbers in the range of $Re \approx 1.1 \times 10^5 - 4.0 \times 10^6$. In this regime, the boundary layer is relatively thick, resulting in a higher tolerance for surface irregularities. Consequently, as-printed LFAM surfaces with standard layer heights (e.g., $k_s \approx 2.0$ mm) often remain close to the hydraulically smooth regime. Furthermore, a distinction must be made regarding the hydrodynamic dominance of the device. For inertia-dominated structures — such as heaving point absorbers or floating platforms — the hydrodynamic loads are primarily governed by radiation and diffraction forces rather than viscous drag. In these specific scenarios, the relative contribution of skin friction to the total hydrodynamic load is often negligible (Palm et al., 2018), suggesting that labour-intensive surface smoothing may not be required. However, for drag-sensitive devices, such as oscillating surge converters or submerged flaps where viscous damping directly opposes the primary motion, the increased friction from LFAM-induced roughness could introduce parasitic damping. In such cases, the trade-off between manufacturing cost and power capture efficiency must be carefully evaluated.

- **Tidal Energy Devices (TEDs):** Tidal turbine blades operate in a transitional to turbulent regime ($Re \approx 4.0 \times 10^5 - 2.0 \times 10^7$) where lift generation is critical. In this zone, even moderate roughness ($k_s \approx 0.5 - 1.0$ mm) causes a distinct deviation from the smooth friction line. Standard LFAM layers will trigger a premature transition to fully rough turbulent flow, increasing drag. For lifting surfaces, this roughness not only increases drag but can severely degrade lift-to-drag ratios (Walker et al., 2014). Therefore, TED blades printed via LFAM might require targeted post-processing to achieve the necessary hydrodynamic efficiency to not affect expected performances.
- **Small Vessels:** Fast-moving displacement or planing hulls operate at high Reynolds numbers ($Re \approx 2.5 \times 10^6 - 9.0 \times 10^8$). In this regime, the friction lines for all plotted LFAM roughness values ($k_s \geq 0.5$ mm) have fully separated from the smooth curve. An untreated LFAM hull ($k_s \approx 4.0$ mm) acts as a "fully rough" plate, causing the friction coefficient to remain at a constant value significantly higher than the smooth baseline. This can result in a drastic friction drag penalty compared to a smooth GRP hull (Demirel et al., 2017). Consequently, filling and fairing appear to be mandatory post-processing steps for LFAM vessels to ensure valid propulsion efficiency.

Out of the limited literature addressing the hydrodynamics of additive manufacturing, this review focuses on a highly representative subset of experimental studies that provide explicit, quantifiable data on skin friction coefficients and layer-induced drag penalties. Several recent studies have evaluated the surface roughness and hydrodynamic drag penalties of desktop-scale polymer and metal AM foils, typically tested in water or wind tunnels at moderate Reynolds numbers (Luznik et al., 2020; De Maio et al., 2023). These foundational investigations highlight that the inherent "staircase effect" of layer-by-layer deposition prematurely triggers boundary layer transition and increases skin friction compared to smooth hydrofoils (De Maio et al., 2023). However, extrapolating these small-scale findings directly to Marine Renewable Energy (MRE) devices or ship hulls presents a significant scaling challenge (Belvisi et al., 2024). At the macro-scale characteristic of LFAM processes like WAAM and BAAM, the geometric amplitude of surface waviness is orders of magnitude larger. Furthermore, marine structures operate at significantly higher realistic Reynolds numbers ($Re > 10^6$), where the boundary layer is fully turbulent and the pronounced macro-roughness elements deeply penetrate the viscous sublayer. Consequently, there is a need to extend the understanding derived from small-scale AM hydrodynamics to establish how the amplified, anisotropic roughness profiles of unprocessed LFAM surfaces uniquely alter flow separation, wake dynamics, and overall drag on large marine structures, thereby highlighting the critical need for scale-specific hydrodynamic modelling.

In scenarios where the inherent macro-roughness of LFAM yields unacceptable hydrodynamic drag for performance-critical applications — such as the hydrofoils of tidal stream turbines or the hulls of high-speed vessels — extensive post-processing becomes mandatory. To mitigate severe drag penalties and prevent phenomena such as premature boundary layer separation or cavitation, the printed surfaces must undergo secondary finishing operations. These typically include CNC machining, abrasive grinding, or the application of marine fairing compounds and epoxy coatings. However, introducing these subtractive or manual finishing steps significantly affect the primary techno-economic advantages of AM. Post-processing proves exceptionally challenging for the complex, topology-optimised geometries frequently targeted by AM. When automated tool access is restricted by intricate curvatures, manufacturers are often forced to rely on highly labour-intensive manual finishing. Because manual finishing is slow and prone to inconsistency, it drastically inflates the final cost of the marine component. Consequently, to keep LFAM economically viable for these demanding hydrodynamic applications, the printing process must be optimised to achieve a "near-net-shape". This means depositing the material as close to its final dimensions and desired surface smoothness as possible right from the start, thereby minimising the need for expensive secondary finishing.

6.2. Effect of print orientation and anisotropy

It is crucial to note that the surface roughness in LFAM is highly anisotropic. The values previously discussed (k_s) represent an equivalent sand-grain roughness (Garg et al., 2024); however, the actual hydrodynamic interaction depends heavily on the orientation of the printed layers (Xiong et al., 2018) relative to the flow direction. The roughness height is geometrically determined by the layer height (L_h) and the local slope of the surface (α) relative to the build plane. The effective step height (h_{eff}) can be approximated as:

$$h_{eff} \approx L_h \cos(\alpha) \tag{4}$$

This geometric definition implies that roughness is maximised on surfaces with shallow slopes relative to the print bed (stair-stepping) and minimised on vertical walls. Furthermore, the drag penalty varies based on the flow alignment:

1. **Longitudinal Alignment (Rails):** When the flow is parallel to the deposition layers (e.g., a hull printed with layers running bow-to-stern), the fluid channels through the grooves. In this "rails" configuration, the effective hydraulic roughness is significantly lower, potentially shifting the performance from the "coarse" curves in Fig. 14 toward the smooth baseline.
2. **Transverse Alignment (Speed Bumps):** When the flow runs perpendicular to the layers, e.g. as discussed by Chivate and Zhou (2024), the fluid must navigate over each layer bead, maximising form drag and turbulence production. This represents the worst-case scenario for roughness penalties.

Therefore, design for marine LFAM must prioritise build orientation not only for mechanical strength but also for hydrodynamics. By orienting components such that critical high-velocity surfaces have layers aligned with the streamlines, manufacturers can significantly mitigate drag penalties without expensive post-processing.

Based on these hydrodynamic evaluations, three core design recommendations are established for the subsequent workflow:

- **Flow-Aligned Deposition:** Whenever kinematically feasible, components should be oriented so that the printed layers align longitudinally with the primary fluid streamlines, minimising transverse form drag.
- **Regime-Specific Finishing:** Labour-intensive post-processing should be strictly reserved for high-Reynolds applications (e.g., tidal blades, planing hulls), whereas inertia-dominated, low-velocity devices (e.g., WEC floaters) can potentially tolerate as-printed finishes.
- **Near-Net-Shape Optimisation:** To preserve the techno-economic benefits of LFAM, the slicing strategy and layer height resolution must be optimised to achieve the required surface tolerance directly during deposition, reducing dependency on secondary machining.

7. Workflow for LFAM of marine components

The implementation of LFAM for marine components necessitates a shift from traditional linear manufacturing workflows. Recent frameworks propose a multi-stage methodology that integrates material science (Khajavi et al., 2021), computational design, and rigorous qualification processes (Chen et al., 2022) to address the unique constraints of the marine environment. The proposed approach, illustrated in Fig. 15, combines technical analysis to facilitate expert-driven decision-making

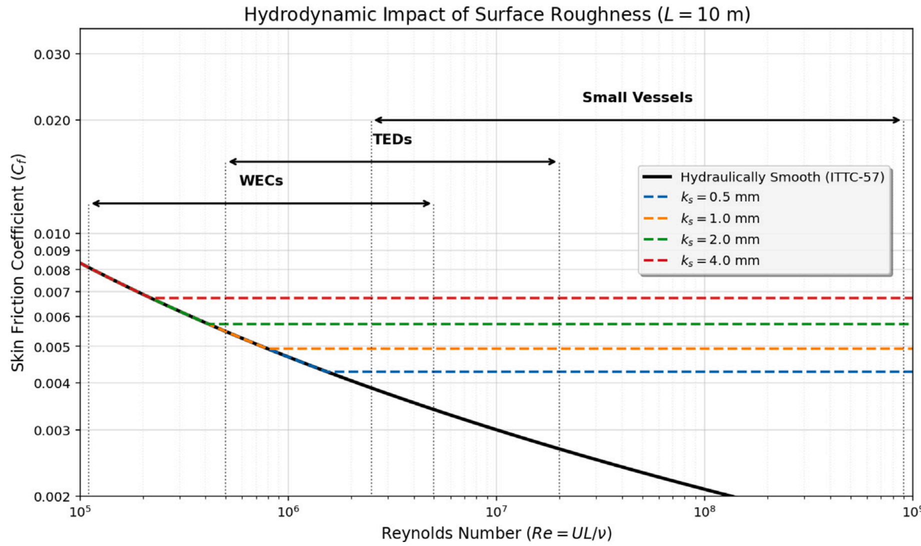

Fig. 14. Hydrodynamic impact of LFAM surface roughness (k_s) on skin friction coefficient (C_f) across Reynolds number regimes. The graph compares the ITTC-57 smooth correlation with roughness penalties for $k_s = 0.5, 1.0, 2.0,$ and 4.0 mm. Operational Reynolds Number ranges for Wave Energy Converters (WECs), Tidal Energy Devices (TEDs), and Small Vessels are indicated by horizontal arrows and vertical delimiters.

Table 5
Proposed LFAM workflow steps to the preceding foundational sections of the review.

Workflow step (Section 7)	Foundational inputs
1. Material & Technology Selection	Section 4 (LFAM Technologies), Section 5 (Materials)
2. Re-design & Optimisation	Section 3 (Structural Loads), Section 4 (Fatigue)
3. Printing Configuration	Section 4 (Kinematics), Section 6 (Orientation/Anisotropy)
4. Post-Processing Configuration	Section 6 (Hydrodynamic Roughness Mitigation)
5. Sample Evaluation	Section 4 (Mechanical Integrity & Fatigue)
6. Printing & Monitoring	Section 4 (Digital Thread & Monitoring)
7. Certification & Compliance	Section 3 (Marine Standards), Section 4 (Class Rules)

to guide development from concept to deployment. The following subsections analyse the critical phases of this workflow, highlighting key challenges and established methodologies identified in recent literature.

The successful implementation of the seven-step workflow detailed in this section relies heavily on the foundational parameters established in the preceding chapters. Specifically, the structural and regulatory constraints (Section 3) dictate the initial performance targets. The selection of robotic kinematics and deposition technologies (Section 4), combined with the specific polymer or metal material properties (Section 5), directly governs the early design and optimisation phases. Furthermore, the hydrodynamic drag penalties associated with layer height and orientation (Section 6) establish the strict requirements for the final post-processing and surface-finishing stages. To improve navigability and demonstrate this interconnectivity, Table 5 maps each workflow step to its corresponding foundational section.

7.1. Material and technology selection

Consequently, established selection frameworks extend beyond conventional mechanical properties to incorporate the severe environmental considerations established earlier, such as corrosion resistance.

Current research emphasises that the foundation of any successful LFAM application lies in the careful selection of both material and additive manufacturing process. Consequently, established selection frameworks extend beyond conventional mechanical properties to incorporate considerations such as corrosion resistance, water absorption, UV degradation, and long-term structural stability in high-humidity and saline environments.

Studies indicate that selecting an LFAM process compatible with a broad range of factors — including, but not limited to, the material's thermal behaviour, deposition rate, inter-layer bonding performance, resolution, and build envelope — is critical (Vicente et al., 2023). For instance, comparative analyses characterise pellet-based extrusion systems as advantageous for their high deposition rates and scalability (1 to 2 orders of magnitude faster than filament systems), though often at the cost of dimensional accuracy and surface finish (Duty et al., 2017). Crucially, this surface limitation must be evaluated against the hydrodynamic regimes discussed in Section 6. As demonstrated in previous Fig. 14, the characteristic roughness of pellet extrusion ($k_s \approx 2$ mm) typically remains within the admissible roughness limit (k_{adm}) for WECs, rendering it a viable, low-cost option. Conversely, for high-Reynolds applications like tidal blades or planing hulls, this same roughness triggers the "fully rough" drag penalties identified in Section 5, necessitating either a higher-resolution technology for post processing or the allocation of budget for extensive surface finishing.

Conversely, WAAM is noted for offering excellent mechanical integrity for metallic structures, yet it demands precise control over thermal gradients (Zhang et al., 2024) and residual stresses to mitigate warping and anisotropy (Wu et al., 2018). These complex interdependencies indicate that it is required the adoption of Multi-Criteria Decision-Making methods, such as decision matrices or scoring frameworks, to balance environmental performance, fabrication feasibility, and application-specific priorities.

Within these frameworks, quantitative performance indicators — such as fatigue strength, cost per kilogramme, and possible printability indexes — might be normalised and weighted according to the functional demands of the marine structure. For example, design strategies for offshore energy components often prioritise fatigue endurance and corrosion resistance (Adedipe et al., 2016), whereas those for aquaculture cages (Chu et al., 2023) tend to emphasise material sustainability, ease of handling, and production speed (Miranda et al., 2025). In

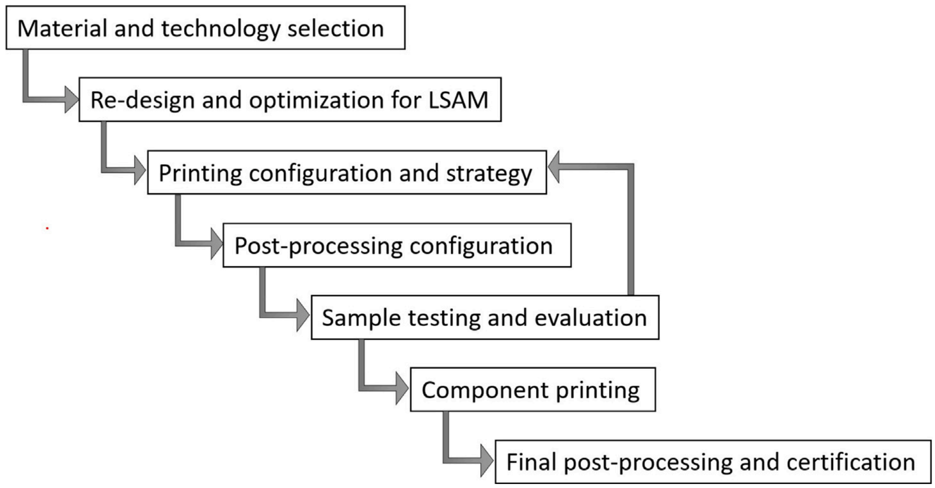

Fig. 15. Ideal workflow for the Large-Format Additive Manufacturing of marine components, backed by recent literature.

all cases a multi-criteria approach is essential to ensure that both functional and operational requirements are adequately addressed.

Furthermore, it is widely recognised that materials conventionally used in marine applications may not be directly transferable to LFAM without significant trade-offs. Research into the anisotropic nature of LFAM-produced parts — where mechanical properties vary significantly between the build direction and in-plane directions — demonstrates the necessity of validating structural performance in all relevant load orientations (Kok et al., 2018). The literature suggests that relying on generic material data is insufficient; instead, the use of detailed datasheets or experimentally derived data for LFAM-processed materials is essential to meet final application requirements. Even commonly accepted materials such as polyamide or stainless steel have been shown to exhibit reduced performance when printed via LFAM due to issues like weak inter-layer adhesion or porosity, reinforcing the need for a critical assessment of material suitability for both the target environment and the chosen process.

7.2. Re-design and optimisation for LFAM

Following material and process selection, the design paradigm adapts to leverage LFAM's unique capabilities. While traditional marine components are constrained by subtractive manufacturing or welding standards — often resulting in conservative, over-engineered forms — LFAM facilitates topology optimisation, integrated features, and geometry simplification (reduced number of separate parts) (Fernández et al., 2021; Mancuso et al., 2022). These capabilities open the door to lighter, stronger, and more sustainable components.

Re-design strategies for LFAM encompass the removal of unnecessary supports, the segmentation of parts into print-compatible subunits, and the adaptation of geometry considering build orientation to minimise distortion and improve mechanical performance. Crucially, the design process accounts for the anisotropic behaviour inherent to additive manufacturing (Kok et al., 2018). Optimisation routines — driven by finite element analysis and algorithmic design — are employed to iteratively improve weight-to-strength ratios and reduce material waste (Giannini et al., 2025).

Moreover, marine-specific design adaptations, such as integrated watertight spaces, water-draining geometries, or novel surface patterns, are incorporated at this stage (Sözen and Neşer, 2025). This re-design phase ultimately transforms LFAM from a mere manufacturing tool into a facilitator of performance-driven innovation.

7.3. Printing configuration and strategy

Following material selection and geometric finalisation, the definition of the LFAM printing strategy constitutes a critical phase in the manufacturing workflow. This stage encompasses the determination of key parameters such as layer height, deposition rate, toolpath planning, build orientation, and thermal control. It is well-established that each of these parameters directly governs the mechanical properties, dimensional accuracy, surface finish, and internal stress distribution of the printed component.

In the context of marine applications, characterised by large-scale components and complex, multi-axial loading, the optimisation of print strategy is paramount for balancing structural performance with process efficiency. Research highlights that build orientation plays a significant role in determining inter-layer bonding quality and mechanical anisotropy. While horizontal builds are noted for reducing print time and simplifying support structures, they are often associated with weaker performance in the vertical axis due to limited inter-layer adhesion (Sun et al., 2020). Conversely, vertical build orientations are utilised to enhance strength in specific load-bearing directions, despite the potential trade-offs regarding longer print times and increased support requirements.

Thermal management represents a primary challenge, especially, in metallic LFAM processes, particularly WAAM, where high deposition rates induce significant residual stresses and thermal gradients. To mitigate these effects, strategies such as inter-pass temperature control, active cooling systems, and substrate pre-heating are frequently employed (Wu et al., 2018). The effectiveness of these measures correlates strongly with the material's thermal conductivity and specific energy input. For metallic components, the integration of advanced print simulation tools allows for the modelling of heat accumulation and the prediction of distortion, enabling the proactive adjustment of process parameters prior to fabrication.

The selection of printing parameters is typically grounded in technical documentation and process guidelines provided by material and equipment manufacturers. These references supply critical baseline data on layer heights, extrusion speeds, minimum wall thicknesses, and temperature envelopes, which serve as prerequisites for ensuring process reliability and print quality (Dahat et al., 2020).

Furthermore, the slicing stage — where 3D geometry is converted into layered toolpaths — is identified as a determinant of the printed part's fidelity relative to its CAD model. The selection of slicing software, resolution settings, infill strategies, and contour algorithms significantly impacts geometric accuracy. Maintaining parts within acceptable tolerances is essential, particularly for mating components or structures intended for tight-fitting marine installations. Techniques such as adaptive slicing and rule-based path planning are explored in current methodologies to improve accuracy and minimise defects (Hu et al., 2022).

Finally, to enhance both mechanical performance and surface quality, advanced strategies such as non-planar printing are increasingly investigated. Unlike traditional planar deposition, non-planar printing utilises curved paths that conform to the component's geometry, thereby reducing stair-stepping effects and improving inter-layer bonding (Chakraborty et al., 2008). This approach is particularly advantageous for curved or hydrodynamically sensitive marine structures, where smooth finishes and isotropic strength distribution are critical requirements.

7.4. Post-processing configuration

Post-processing in LFAM is defined not as an optional step but as a fundamental requirement, particularly within marine applications where dimensional tolerances, surface roughness, and fatigue life are critical performance metrics. This phase comprises a diverse array of treatments, ranging from heat treatments and shot peening to surface machining and coating application. The definition of the post-processing strategy is inherently driven by the interaction between the specific material properties and the functional operational envelope of the component.

For instance, metallic components such as WAAM-produced steel mooring brackets typically require post-build stress-relieving heat treatments, followed by precision CNC machining of bolted interfaces to meet tolerance and surface finish specifications. In contrast, thermoplastic structures like aquaculture panels fabricated via pellet-fed extrusion generally necessitate surface smoothing and the application of UV-protective coatings to ensure long-term durability. For MRE devices, and specifically floating hull components, post-processing protocols frequently incorporate fibreglass reinforcement, protective coatings, and antifouling systems to mitigate biofouling (Keeley et al., 2021).

Standard methodologies dictate that post-processing constraints be integrated into the early design and manufacturing phases to guarantee compatibility with part geometry, material behaviour, and functional objectives. Additionally, the sustainability impact of post-processing is a key consideration; excessive finishing operations risk diminishing the environmental benefits associated with LFAM (Dias et al., 2022). Accordingly, surface finish criteria are balanced against durability requirements, with novel finishing techniques — such as robotic polishing or eco-friendly coatings — being leveraged to optimise the production footprint.

7.5. Sample printing and evaluation

Closely linked to the definition of post-processing protocols is the validation phase. Before proceeding to full-scale printing, the production of test parts or full subcomponents is established as a critical prerequisite. These samples serve the dual purpose of validating material-process compatibility and calibrating post-processing routines. In marine contexts, accelerated corrosion and fatigue testing are prioritised to derive insights into long-term performance under aggressive conditions (Ermakova et al., 2022). Furthermore, the validation of active mechanical components can be accelerated using robotised dry test rigs to emulate hydrodynamic responses, bridging the gap between numerical models and costly wave tank deployments (Salar et al., 2026).

Evaluation protocols typically encompass tensile, flexural, and impact strength assessments, complemented by advanced inspection techniques such as CT scanning or microscopy for the analysis of inter-layer bonding and porosity (Du Plessis et al., 2018). Mechanical performance is benchmarked against theoretical design values and relevant regulatory standards (e.g., DNV, ABS). Ultimately, the quantitative feedback derived from this testing drives a closed-loop refinement of print strategies, process parameters, and part geometries, ensuring that performance deviations are rectified before resources are committed to the final build.

7.6. Component printing and monitoring

Following the design and the printing process validation, the execution of the final print represents the materialisation of the LFAM workflow. Process stability and quality control during this phase is identified as primary determinants of component integrity, particularly for assets intended for high-risk marine environments. Consequently, industrial implementation relies on advanced monitoring architectures — encompassing optical systems for computer vision, thermal imaging, and in-situ sensors — to track print fidelity in real-time. These systems facilitate the early detection of deviations in thermal profiles, bead geometry, or material deposition, establishing a closed-loop control mechanism that mitigates defect formation (Franke et al., 2025).

The paradigm of process monitoring in LFAM is shifting from passive data logging to active, AI-driven quality assurance. Recent literature highlights that the volume and complexity of data generated during large-scale deposition — ranging from thermal histories to layer-wise geometric profiles — exceed the capabilities of traditional statistical process control (Ye et al., 2025). Consequently, Deep Learning (DL) architectures, particularly Convolutional Neural Networks (CNNs), have emerged as the dominant methodology for real-time defect classification. Studies demonstrate that CNN-based models trained on in-situ optical, thermal, and acoustic imagery can identify surface anomalies, such as lack of fusion or unstable bead geometry in DED and WAAM processes, with accuracies frequently exceeding 95% (Cao et al., 2023). Furthermore, the focus is expanding towards multi-sensor fusion, where cross-attention neural networks and machine learning algorithms correlate heterogeneous data streams (e.g., acoustic emissions, melt-pool temperature, and arc voltage) to predict internal microstructural properties that are invisible to optical sensors. This in-situ prediction capability is critical for LFAM, as it allows for the interception of defects before they propagate through subsequent layers. More recent advancements propose the integration of these AI models into closed-loop control systems. By utilising anomaly-driven Reinforcement Learning (RL), systems can now autonomously adjust process parameters — such as travel speed or material feed rate — in response to detected anomalies, effectively minimising the need for post-process rework and facilitating the certification of large marine structures (Dharmadhikari et al., 2023; Schürmann et al., 2025).

In the marine sector, digital traceability is aligning with emerging regulatory frameworks for safety-critical and load-bearing components. The aggregation of metadata — including process parameters, environmental conditions, and sensor logs — into a comprehensive "digital thread" is becoming a prerequisite for certification by classification societies.

Furthermore, the substantial scale of marine components drives the adoption of specific logistical strategies. Decentralised manufacturing models, including on-site or near-site fabrication using mobile LFAM platforms, are utilised to minimise transportation constraints and simplify integration into larger offshore systems (Kostidi and Nikitakos, 2024). Within these distributed manufacturing scenarios, cross-site consistency is maintained through rigorous printer calibration protocols and standardised operating procedures.

Ultimately, the fabrication phase serves as the physical convergence of material selection, design adaptation, and process configuration. It functions not as the conclusion of the workflow, but as the precursor to the mandatory stages of final qualification and compliance verification.

7.7. Final post-processing and certification

Following the additive manufacturing process, the component undergoes a defined sequence of post-processing procedures tailored to meet functional, structural, and regulatory mandates. These operations range from precision CNC machining, required to achieve critical mating tolerances, to the application of surface treatments such as anti-UV coatings or sealants. Mechanical finishing steps are systematically employed to improve surface integrity and mitigate stress concentration factors that serve as initiation points for fatigue failure (Pegues et al., 2018).

Compliance verification relies on the implementation of comprehensive quality control protocols. Standard methodologies encompass dimensional inspections utilising 3D laser scanning, surface roughness characterisation, and Non-Destructive Testing (NDT) methods including ultrasonic inspection, X-ray, or dye penetrant testing—selected based on material properties and component criticality (Honarvar and Varvani-Farahani, 2020).

Certification regimes for marine and offshore components are governed by stringent standards established by classification societies such as DNV, ABS, or Lloyd's Register (Junghans et al., 2020) (See also previous Section 3.3). As previously discussed, achieving this compliance now directly relies on adherence to their recently established and updated, AM-specific frameworks, specifically DNV-ST-B203, the ABS Requirements for Additive Manufacturing, and the LR Guidance Notes for AM parts. These bodies impose rigorous requirements regarding material traceability, process repeatability, and mechanical performance. Conformance increasingly necessitates the submission of a "digital thread", which is a comprehensive data package comprising material certificates, process logs, in-situ sensor data, and post-build inspection reports.

Beyond structural certification, operational readiness is achieved through the application of environment-specific protective measures. These strategies include the deployment of antifouling coatings to resist marine growth, hydrophobic treatments to minimise hydrodynamic drag, and cathodic protection systems designed to prevent galvanic corrosion in multi-material assemblies.

This final phase functions as the consolidation of all upstream engineering decisions, transitioning the LFAM-printed structure from a digitally conceived prototype to a qualified, operational marine asset. Furthermore, it closes the decision-making loop by generating performance data that informs the refinement of the methodology for future manufacturing iterations.

8. Performance and cost metrics

8.1. Project-level metrics

The formulas presented in this subsection are utilised by project developers and investors to estimate the macro-scale financial viability of marine deployments, allowing for direct cost comparisons between entire LFAM-manufactured arrays and conventional offshore farms.

The viability of marine structures and MRE devices depends not only on their structural integrity or hydrodynamic performance, but also on their economic feasibility in terms of production cost and commercial scaling. Recent literature indicates that the adoption of LFAM can drive significant economic efficiencies, with reported production cost reductions reaching up to 30%–50% compared to conventional subtractive or formative methods (Vicente et al., 2023). These figures typically represent isolated or aggregated industrial case studies rather than formal statistical averages. However, it is critical to note that such margins are highly variable and contingent upon a complex interplay of factors, including component topology, physical dimensions, production batch size, material costs, and the extent of required post-processing.

Given this variability, an effective cost advantage cannot be assumed a priori; rather, it must be verified through rigorous quantitative analysis specific to the target application. To facilitate such comparative evaluations, a set of standard techno–economic metrics is typically employed to benchmark LFAM against traditional fabrication strategies. These include capital expenditure (CapEx), operational expenditure (OpEx), levelised cost of energy (LCOE), estimated cost per unit (ECU), and discounted payback period (DPP). These indicators, routinely applied in the evaluation of ships, offshore platforms, and MRE converters, provide the necessary quantitative basis for early-stage decision-making regarding the selection of fabrication methods.

8.1.1. Capital expenditures (CapEx) and cost breakdown

Capital expenditure (CapEx) represents the total upfront investment required to bring a marine energy project to operational status. For a single device or an entire array, CapEx can be decomposed into several cost components (Morthorst and Kitzing, 2016). This breakdown is formalised as:

$$\mathrm{CapEx} = C_{\mathrm{dev}} + C_{\mathrm{BoP}} + C_{\mathrm{inst}} + C_{\mathrm{EPM}} + C_{\mathrm{log}} + C_{\mathrm{cont}} + C_{\mathrm{decom,res}}, \tag{5}$$

Each term corresponds to a specific cost centre. Specifically, C_{dev} represents device manufacturing and assembly, including the fabrication of the energy converter, while C_{BoP} accounts for the balance-of-plant, such as foundations, moorings, electrical infrastructure, and other supporting systems. The term C_{inst} covers installation and commissioning, detailing offshore deployment activities, and C_{EPM} encompasses engineering, procurement, and project management services. Additionally, C_{log} captures the costs associated with transportation and logistics. To account for financial uncertainties and required upgrades, C_{cont} provides necessary contingency allowances. Finally, $C_{\mathrm{decom,res}}$ is allocated for decommissioning reserves, which encompass end-of-life obligations, retrofits, and provisions for the device's life extension (Nguyen et al., 2020).

At the device level, the *Estimated Cost per Unit* (ECU) aggregates these same categories on a per-device basis (Giannini et al., 2022):

$$\mathrm{ECU} = C^{(1)}_{\mathrm{dev}} + C^{(1)}_{\mathrm{BoP}} + C^{(1)}_{\mathrm{inst}} + C^{(1)}_{\mathrm{EPM}} + C^{(1)}_{\mathrm{log}} + C^{(1)}_{\mathrm{cont}}, \tag{6}$$

where the superscript (1) indicates that the cost is allocated per individual unit. This metric is particularly useful for comparing different device designs or scaling scenarios. A further normalisation is provided by the *Estimated Cost of Technology per MW* (ECT), which relates total CapEx to the installed capacity:

$$\mathrm{ECT} = \frac{\text{Total CapEx}}{P_{\mathrm{inst}}} \quad [\text{currency/MW}], \tag{7}$$

where P_{inst} is the nameplate (installed) capacity in megawatts. This allows for direct comparison across technologies with different power ratings.

8.1.2. Operational expenditures (OpEx)

Operational expenditures (OpEx) encompass all recurring costs incurred during the operational life of the project. These include scheduled and unscheduled maintenance, offshore servicing campaigns, insurance premiums, leasing fees, environmental monitoring, and onshore support operations. The annual OpEx in year t is denoted as $C_{\mathrm{op},t}$. In many techno–economic models, a constant real annual OpEx is assumed, such that $C_{\mathrm{op},t} = C_{\mathrm{op}}$ for all t.

8.1.3. Annual energy production (AEP) and capacity factor

The annual energy production (AEP) quantifies the net amount of electricity generated by the system over a year. For a general MRE device is calculated as:

$$\mathrm{AEP} = P_{\mathrm{inst}} \cdot \mathrm{CF} \cdot 8760 \cdot (1 - L), \tag{8}$$

where P_{inst} is the installed capacity in MW, CF is the net capacity factor (a dimensionless ratio between 0 and 1), and 8760 is the number of hours in a year. The term L represents aggregated losses due to availability issues, curtailment, electrical inefficiencies, and array effects. This formulation provides a realistic estimate of the useable energy output, accounting for both technical and operational constraints.

For WECs, the mean AEP is typically calculated using a performance matrix approach, whereby device power output is correlated with discrete sea states bins weighted by their occurrence frequency in an average year. This method offers a favourable balance between computational efficiency and fidelity, as detailed by Kofoed and Folley (2016).

In the context of TEDs, AEP estimation methods can handle truncated input data by leveraging the periodic nature of tidal resources.

The International Electrotechnical Commission (IEC) suggests that at least 90 days of data can suffice to estimate AEP, with uncertainty quantification based on record length and tidal variability (Balestrino et al., 2019; Xu et al., 2023).

8.1.4. Levelised cost of energy (LCOE)

The levelised cost of energy (LCOE) is a widely used metric that expresses the average cost per unit of electricity generated over the lifetime of the project, discounted to present value. This is a useful metric in the context of the development of MRE or hybrid marine energy devices. It is defined as:

$$\mathrm{LCOE} = \frac{\sum_{t=0}^{n} \frac{I_t + O_t + F_t + D_t}{(1+r)^t}}{\sum_{t=1}^{n} \frac{E_t}{(1+r)^t}}, \tag{9}$$

In this expression, I_t represents capital expenditures in year t, O_t are operation and maintenance costs, F_t are fuel costs (typically negligible for wind, wave and tidal energy), D_t are decommissioning costs, and E_t is the net energy produced in year t. The discount rate is denoted by r (typically 6%–10% for MRE applications), and n is the project lifetime in years (generally 20–25 years) (Branker et al., 2011). Because the final LCOE value is highly sensitive to the chosen discount rate and inherent uncertainties in early-stage capital expenditures, parametric sensitivity analyses represent a standard engineering practice to establish credible cost bounds when evaluating novel additive manufacturing methods.

For simplified cases where OpEx and energy production are constant over time, and all CapEx is incurred at $t = 0$, the LCOE can be approximated using the capital recovery factor (CRF):

$$\mathrm{LCOE} \approx \frac{\mathrm{CapEx} \cdot \mathrm{CRF}(r, n) + O}{E}, \qquad \mathrm{CRF}(r, n) = \frac{r(1+r)^n}{(1+r)^n - 1}. \tag{10}$$

This form is particularly useful for preliminary assessments and parametric studies.

8.1.5. Payback period

The payback period is another key economic indicator, relevant to LFAM, representing the time required for the project to recover its initial investment. The *simple payback period* is defined as the smallest integer N such that the cumulative net cash inflow equals or exceeds the initial CapEx:

$$\sum_{t=1}^{N} C_t^{\mathrm{net}} \geq \mathrm{CapEx}. \tag{11}$$

A more rigorous version is the *discounted payback period* (DPP), which accounts for the time value of money:

$$\mathrm{DPP} = \min \left\{ N \;\middle|\; \sum_{t=1}^{N} \frac{C_t^{\mathrm{net}}}{(1+r)^t} \geq \mathrm{CapEx} \right\}. \tag{12}$$

This metric is particularly relevant for investors and stakeholders evaluating the financial risk and return profile of MRE plants.

8.2. Part-level material and energy estimation

At the micro-economic level, the following equations are employed by manufacturing engineers on the shop floor to accurately predict the mass, raw material requirements, and electricity consumption of individual printed components prior to initiating the print job, Table 6. LFAM, typically involving build volumes of 1 m^3 or greater, requires a comprehensive evaluation of both material usage and energy consumption. These estimations are essential for assessing production costs, environmental sustainability, and overall life-cycle performance. The following subsections present a set of analytical expressions used to estimate material mass, electricity consumption and energy-related costs.

8.2.1. Material mass estimation

The mass of a printed part can be estimated using the following expression:

$$m_{\mathrm{part}} = \rho, V_{\mathrm{solid}}, f_{\mathrm{infill}} \tag{13}$$

In this equation, ρ denotes the density of the printing material, expressed in kilogrammes per cubic metre (kg/m^3). The term V_{solid} refers to the nominal volume of the part as defined in the CAD model, assuming a fully solid geometry.

The infill factor f_{infill} is a dimensionless quantity ranging from 0 to 1, representing the proportion of the internal volume that is actually filled with material. For example, an infill of 0.5 implies that only half of the internal volume is occupied. This formula allows for a realistic estimation of the printed mass by scaling the theoretical solid mass according to the chosen infill percentage. Such expression is normally implemented in common 3D printing software to estimate required material and printing time, e.g. Manford et al. (2022).

8.2.2. Electricity consumption per print

The energy required to deposit material during the printing process is commonly quantified using the specific electricity consumption (SEC), which measures the energy used per kilogramme of deposited material. The total electricity consumed during the printing phase is given by:

$$E_{\mathrm{print}} = E_{\mathrm{SEC}} \cdot m_{\mathrm{part}} \tag{14}$$

Here, E_{SEC} is the specific electricity consumption in kilowatt-hours per kilogramme (kWh/kg), and m_{part} is the mass of the printed part. Empirical data show that polymer-based LFAM typically exhibit SEC values between 0.1 and 0.5 kWh/kg (Chen et al., 2024), representing a range derived from multiple large-format printing samples, with an established median of approximately 0.24 kWh/kg. In contrast, metal-based WAAM processes are significantly more energy-intensive, with reported SEC values ranging from 2.3 to 2.7 kWh/kg (Bekker and Verlinden, 2018; Marqués et al., 2024), primarily based on individual life-cycle assessment case studies rather than pooled statistical data.

8.3. Auxiliary electricity consumption

In addition to the energy used for material deposition, LFAM systems consume electricity through auxiliary operations. These include pellet drying, HVAC systems, idle power draw, and inter-pass cooling. The total electricity consumption for a complete print job is therefore:

$$E_{\mathrm{job}} = E_{\mathrm{print}} + E_{\mathrm{aux}} \tag{15}$$

In this expression, E_{job} represents the total energy consumed for the job, combining both the printing phase (E_{print}) and auxiliary systems (E_{aux}). Depending on the process and environmental conditions, auxiliary loads can be substantial. For instance, conditioned build chambers or the use of hygroscopic materials requiring pre-drying may significantly increase E_{aux}.

8.4. Smart-manufacturing aspects and dynamic energy costs

To capture the complexities of modern energy markets, these formulas allow facility managers to integrate dynamic electricity pricing into their manufacturing schedules, optimising energy-intensive printing phases eventually to coincide with off-peak tariff windows.

Standard techno-economic models for additive manufacturing typically quantify energy costs using a static average price, calculated as the product of total energy consumption and a fixed unit rate:

$$C_{\mathrm{energy}} = p_{\mathrm{elec}} \cdot E_{\mathrm{job}} \tag{16}$$

Here, p_{elec} denotes the electricity price per kilowatt-hour (€/kWh), and E_{job} represents the total energy consumed. While sufficient for

Table 6
Summary of LFAM energy and cost estimation formulas.

Formula	Description
$m_{part} = \rho V_{solid} f_{infill}$	Printed part mass
$E_{print} = E_{SEC} \cdot m_{part}$	Electricity for deposition
$E_{job} = E_{print} + E_{aux}$	Total job electricity
$C_{energy} = p_{elec} \cdot E_{job}$	Energy cost
$E_{job} = \sum_k P_k t_k$	Real time energy assessment

small-scale rapid prototyping, this static approach often proves inadequate for LFAM of marine structures. Review of production logistics indicates that fabrication cycles for large marine components — such as turbine blades or hull sections — frequently extend over multiple days (Post et al., 2021). Consequently, the manufacturing process inevitably intersects with varying grid-level tariff structures (e.g., peak, off-peak, or dynamic spot-market rates). Under these conditions, utilising a fixed average price fails to capture the significant economic impact of temporal price volatility. To resolve these discrepancies, more robust economic models propose expanding the cost function into the time domain. This approach integrates the instantaneous power demand of the LFAM system — which fluctuates based on process states such as heating, extrusion, or cooling — with dynamic pricing structures:

$$C_{energy} = \int_0^{T_{build}} P(t) \cdot p_{elec}(t), dt \tag{17}$$

where:

- T_{build} represents the total duration of the print job (h).
- $P(t)$ is the instantaneous power consumption (kW) at time t.
- $p_{elec}(t)$ is the time-dependent electricity price (€/kWh).

In computational practice, this integral is approximated using a discrete summation over slicing steps or time intervals (Δt_i):

$$C_{energy} \approx \sum_{i=1}^{N} P_i \cdot p_{elec,i} \cdot \Delta t_i \tag{18}$$

This dynamic formulation is critical for accurate Lifecycle Cost Analysis in the marine sector. It enables the implementation of "smart manufacturing" strategies (Karimi et al., 2021), where energy-intensive phases — such as solid infill deposition — can be algorithmically scheduled to coincide with low-cost tariff windows.

8.5. Direct power–time measurement and final process efficiency

Alternatively, for higher-resolution energy accounting, a direct measurement approach can be preferred. If the average power draw of each subsystem is known, the total energy consumption can be calculated as:

$$E_{job} = \sum_k P_k, t_k \tag{19}$$

In this formulation, P_k is the average power consumption of subsystem k (in kW), and t_k is the duration of its operation (in hours). This method enables disaggregation of energy usage across different subsystems—such as extrusion, motion control, cooling, and idle states.

The values shown in Table 7 highlight a clear difference in energy intensity between polymer-based LFAM and metal-based WAAM processes. LFAM systems tend to be one order of magnitude less electricity-intensive. However, auxiliary energy consumption (E_{aux}) can be significant, particularly when using hygroscopic pellets that require drying or when operating in climate-controlled environments. In WAAM, non-arc energy loads such as interpass cooling and fume extraction fans are often important contributors (Bekker and Verlinden, 2018). For this reason, it is essential to clearly indicate whether SEC values include auxiliary consumption, to avoid underestimating the total energy demand.

Concerning techno-economic and sustainability assessments of LFAM, recent Life Cycle Assessment (LCA) and energy-assessment studies provide critical quantitative benchmarks. For polymer-based systems, real-time industrial-scale data acquisition on LFAM platforms has quantitatively established their high energy efficiency. By mapping electricity usage across diverse printing jobs, these systems exhibit clearly lower SEC than standard desktop material extrusion networks (Chen et al., 2024). Furthermore, the environmental footprint is substantially lowered when bypassing energy-intensive intermediate steps, such as filament extrusion. Direct pellet-fed large-format systems utilising upcycled biomass waste, such as spent coffee grounds compounded with polyolefins, validate both structural integrity and a drastic reduction in processing stages (Romani et al., 2024). The operational efficiency of these systems can be further enhanced through explainable artificial intelligence (AI), which quantitatively links machine printing parameters to explicit LCA impacts, demonstrating how targeted parameter optimisation directly mitigates overall electricity consumption (Zhu et al., 2026).

In the domain of metallic LFAM, WAAM, as well, demonstrates highly favourable energy metrics. Recent quantitative analyses correlate deposition rates with SEC, proving WAAM to be the most energy-efficient metallic additive manufacturing process currently available for heavy structural components (Balidas et al., 2024). This is corroborated by direct industrial case studies; for instance, the fabrication of heavy Inconel 625 impellers via WAAM reduced energy consumption threefold and cut material waste from 85% to 35% when compared to conventional subtractive machining (Sword et al., 2024). Prospective LCAs modelling the future industrial scaling of WAAM project up to a 74% reduction in overall environmental impacts, while also identifying argon shielding gas as the primary remaining contributor to the process's ecological footprint (Spreafico et al., 2026). However, it is imperative to maintain a balanced perspective, as pre- and post-processing stages can heavily skew these benefits. Critical assessments reveal that the extensive CNC machining required to achieve final tolerances on WAAM-deposited Ti-6Al-4V can trigger up to 25% higher fossil energy consumption and a 32% higher climate change impact than manufacturing the exact same part from conventional wrought alloys (Lotwala et al., 2025), thereby underscoring the absolute necessity of achieving near-net-shape deposition to truly realise the proposed sustainability goals.

9. Additional key concepts and discussion

LFAM introduces a paradigm shift in the design-to-manufacturing workflow, particularly for marine applications. Unlike traditional fabrication methods, which often involve several stages (Murdy et al., 2021) and exponentially rising costs with increased geometric complexity, LFAM enables the direct fabrication of complex, performance-driven geometries with minimal tooling and setup. This opens the door to advanced design strategies, such as topology optimisation (also using filling structural patterns e.g. Zheng et al. (2019)) and bio-inspired structures, which can now be realised at scale. To support such a trend, examples of new structures are provided by optimised metal components (Yang et al., 2024) and new possible ship structures (Armanfar et al., 2024).

Despite these advantages, several challenges remain. One of the most pressing is the absence of standardised guidelines and certification protocols for LFAM components in marine environments. This gap hinders broader adoption, particularly for safety-critical applications. Additionally, there is limited empirical data on the long-term performance of LFAM-fabricated parts under real marine exposure, including corrosion, fatigue, and biofouling.

Process reliability and quality assurance are also areas of active research. Variability in deposition quality, thermal gradients, and residual stresses can affect part integrity. Emerging solutions include the integration of machine learning algorithms and computer vision systems

Table 7
Reported SEC values for LFAM processes.

Process	SEC [kWh/kg]	Reference
LFAM (polymer, pellet-fed)	0.10–0.50 (median 0.24)	Chen et al. (2024)
Generic WAAM LCA (approx.)	2.46	Shah et al. (2023)
WAAM (stainless steel, 1 kg/h)	2.72	Bekker and Verlinden (2018)

for real-time monitoring and control of extrusion parameters. Post-process verification using 3D scanning technologies offers a scalable approach for dimensional and surface quality assessment, especially in high-throughput production scenarios.

Scalability is another key advantage. Robotic systems mounted on rails or gantries can extend the build volume, while conveyor-based print beds allow for continuous, unattended production. These innovations support the transition from prototyping to industrial-scale manufacturing.

Sustainability considerations are also gaining traction. The use of recycled or circular materials in LFAM is technically feasible, though currently limited by high costs and certification barriers. A more mature supply chain could significantly reduce these constraints and enhance the environmental performance of LFAM processes.

Finally, for new components development and manufacturing, a closed-loop workflow between design, process parameters, and material characterisation is essential. Iterative testing of printed samples ensures that mechanical and environmental performance targets are met, enabling the refinement of both digital models and manufacturing settings.

9.1. Emerging trends and future scenarios

To fully realise the potential of LFAM in the marine sector, future development is anticipated to progress along several critical emerging trends:

- **Standardisation, AI-supported qualification, and digital traceability:** The establishment of dedicated certification protocols for LFAM components is critical. A plausible near-term application includes the qualification of secondary structures, which will pave the way for the mid-term goal of producing the first class-approved primary load-bearing structures. This will rely heavily on robust digital traceability to ensure transparent compliance with classification societies.
- **Integration with smart manufacturing, closed-loop process control, and digital threads:** The adoption of multi-sensor fusion will enable real-time defect correction. For example, deploying closed-loop AI control during WAAM deposition can autonomously ensure the structural integrity of complex geometries, simultaneously generating the complete digital thread required by regulators for the certification of mission-critical assets.
- **Circular feedstocks and recycled materials:** Transitioning to sustainable feedstock streams is essential for minimising life-cycle environmental impacts. Concrete applications include the fabrication of large-scale, modular WEC floaters or aquaculture infrastructure using reinforced, end-of-life maritime plastics or recycled thermoplastic pellets.
- **Hybrid manufacturing routes and mobile LFAM:** Decentralised manufacturing models will overcome the logistical constraints associated with transporting massive marine structures. Future scenarios envision mobile LFAM robotic units and hybrid manufacturing routes — combining additive deposition with automated subtractive finishing — deployed directly at shipyards, ports, or offshore hubs for rapid, on-demand fabrication and repair.

To provide a structured overview of the immediate hurdles and the corresponding pathways forward, Table 8 explicitly maps the main technological challenges in marine LFAM against current research priorities. This synthesis highlights how issues such as anisotropic material behaviour, harsh environmental exposure, and the lack of consolidated standardisation require targeted, multi-disciplinary research efforts (Kok et al., 2018; Junghans et al., 2020; Liu et al., 2026).

10. Conclusion

This paper covers a set of trends and a comprehensive framework for applying Large-Format Additive Manufacturing (LFAM) for marine components, including both thermoplastic and metal-based technologies. Key aspects and methods, not limited to offshore requirements, overview of major LFAM technologies, materials, and economic metrics have been reviewed. The major findings of this review are summarised as follows:

- **Materials Evaluation:** A focused evaluation of materials has identified a subset of polymers and metals particularly suited for marine use with focus to components of marine renewable devices and small vessels. These include fibre-reinforced thermoplastics for structural applications and corrosion-resistant metals such as nickel–aluminium bronze, stainless steels, and titanium alloys for submerged or load-bearing components. These materials offer a balance of mechanical performance, durability, and environmental resistance.
- **Hydrodynamic Efficiency:** The critical role of surface roughness was evaluated based on indicative quantitative figures. The analysis distinguishes between flow regimes: while "as-printed" surfaces may suffice for diffraction-dominated structures like Wave Energy Converters operating at lower Reynolds numbers ($Re < 4.0 \times 10^6$), post-processing strategies are identified as mandatory for high-Reynolds applications — such as tidal blades ($Re \approx 4.0 \times 10^5 - 2.0 \times 10^7$) and fast vessels ($Re \approx 2.5 \times 10^6 - 9.0 \times 10^8$) — to mitigate significant high skin friction implying drag penalties.
- **Workflow Development:** By aligning LFAM capabilities with the specific demands of marine structures, a structured 7-step workflow has been identified that synthesises methodologies applied in recent works—ranging from material selection and design optimisation to post-processing and quality verification. This framework underscores that every phase, from the initial material-technology pairing to the final certification, is equally critical. Ultimately, the systematic execution of these steps ensures that manufactured components attain the requisite quality standards to guarantee reliability and survivability in challenging offshore environments.

The adoption of LFAM in marine engineering has far-reaching implications. It enables greater design freedom, reduces manufacturing complexity, and supports sustainability through the potential use of recycled materials. Moreover, LFAM facilitates rapid prototyping and iterative development, which is especially valuable in emerging sectors like marine renewable energy.

The shift toward digital, automated manufacturing is crucial for meeting growing demands for sustainability, performance, and cost-efficiency. Traditional methods are limited in design flexibility, rapid iteration, and integrated hybrid designs, particularly in customised or low-volume production settings. LFAM overcomes these challenges, offering on-demand production, easy design modifications, and improved material utilisation. These advantages are particularly important for new MRE device concepts that still require significant R&D to

Table 8
Summary of main technological challenges and research priorities for LFAM in marine engineering applications.

Theme	Technological challenges	Research priorities
Material Durability & Environment	Z-axis anisotropy, water absorption, UV degradation, and biofouling impact on inter-layer bonds.	Long-term characterisation of printed polymers and WAAM alloys in seawater; development of marine-specific protecting coatings. (Stankovic et al., 2024; Ermakova et al., 2022)
Process Stability & Quality Assurance	Thermal distortion in WAAM, inconsistent bead geometry, and internal porosity acting as fatigue initiators.	Integration of multi-sensor fusion and AI-driven closed-loop control for real-time defect correction during deposition. (Love et al., 2025; Liu et al., 2026)
Hydrodynamics & Surface Finish	High drag penalties caused by layer-induced surface roughness ("stair-stepping") in high-Reynolds flows.	Optimisation of non-planar printing toolpaths to align with fluid streamlines; automated, low-cost robotic finishing techniques. (Chivate and Zhou, 2024; Wu et al., 2018)
Certification & Standardisation	Absence of marine-specific LFAM class-society rules; difficulty in validating massive, monolithic structures.	Establishment of robust "digital thread" protocols; derivation of acceptable safety factors and NDT frameworks for printed parts. (Junghans et al., 2020; Honarvar and Varvani-Farahani, 2020)

reach higher technology readiness levels. Using LFAM could maintain R&D costs low, enabling fast progress to higher TRLs. However, the realisation of these advantages is not automatic; suitable economic metrics—such as those reviewed in this work—are required to quantitatively evaluate the comparative benefit of LFAM versus traditional manufacturing. Similarly, rigorous assessment is essential to substantiate anticipated potential environmental benefits of opting for LFAM regarding pollution reduction and sustainability.

While this study centred on polymeric and metallic workflows, concrete-based materials LFAM represents a growing area of interest. This technology was not detailed in the current review due to its nascent phase within the marine environment, where peer-reviewed case studies and data on long-term resilience are currently limited. Additionally, questions regarding the comparative sustainability of marine-grade printable concrete remain to be addressed. As the technology matures, however, future work should specifically investigate concrete LFAM to assess its potential role in fabricating gravity-based foundations and coastal infrastructure.

Ultimately, this study serves to support both the theoretical and practical domains of applied ocean research. From a theoretical perspective, the work offers a preliminary baseline that directly links marine environmental constraints—such as hydrodynamic drag and seawater corrosion—to specific LFAM material selection and process parameters. Practically, the proposed workflow benefits the ocean engineering industry by providing a systematic pathway to reduce lead times, lower prototyping costs for low-TRL MRE devices or other marine structures, and implement decentralised, circular manufacturing strategies directly at shipyards and offshore sites.

Future research should prioritise the validation of LFAM-fabricated components under real-world marine conditions, including long-term exposure to saltwater, mechanical fatigue, and bio-fouling. Industrial-scale pilot projects will be essential to assess scalability, process stability, and cost-effectiveness. Additionally, the development of a comprehensive material-process-performance database will be critical to support informed decision-making and accelerate the integration of LFAM into mainstream marine manufacturing.

CRediT authorship contribution statement

Gianmaria Giannini: Writing – original draft, Visualization, Resources, Project administration, Methodology, Investigation, Funding acquisition, Formal analysis, Data curation, Conceptualization. **Giuseppe Giorgi:** Writing – review & editing, Methodology, Funding acquisition. **Giuliana Mattiazzo:** Writing – review & editing, Supervision, Funding acquisition. **Giovanni Avallone:** Writing – review & editing. **Paulo Rosa-Santos:** Writing – review & editing. **Francisco Taveira-Pinto:** Writing – review & editing.

Declaration of Generative AI and AI-assisted technologies in the writing process

During the preparation of this work the authors used Microsoft Copilot and Google Gemini in order to improve paper flow and for formatting reasons. After using these tools, the authors reviewed and edited the content as needed and take full responsibility for the content of the publication.

Declaration of competing interest

The authors declare that they have no known competing financial interests or personal relationships that could have appeared to influence the work reported in this paper.

Acknowledgements

This study was made possible thanks to funding from the European Research Executive Agency (REA) under the European Union's Horizon Europe research and innovation programme through the Marie Skłodowska-Curie grant agreement No. 101206509 - Project: Progressing Wave Energy Conversion via Large-Scale Additive Manufacturing (WEC-Pro). Additional support was previously provided through the Stimulus of Scientific Employment program of the Portuguese Fundação para a Ciência e a Tecnologia (FCT), under the individual grant reference 2022.04954.CEECIND/CP1728/CT0007. Some of the images relative to WEC technologies are provided by Marine Offshore Renewable Energy (MOREnergy Lab), Politecnico di Torino, these are distributed under a Creative Commons Attribution-ShareAlike 4.0 License.

References

Abbate, C., Giorgianni, C., Brecciaroli, R., Giacobbe, G., Costa, C., Cavallari, V., Albiero, F., Catania, S., Tringali, M.A., Martino, L.B., Abbate, S., 2006. Changes induced by exposure of the human lung to glass fiber–reinforced plastic. Environ. Health Perspect. 114, 1725–1729. http://dx.doi.org/10.1289/ehp.8676, URL https://www.ncbi.nlm.nih.gov/pmc/articles/PMC1665410/.

Adedipe, O., Brennan, F., Kolios, A., 2016. Review of corrosion fatigue in offshore structures: Present status and challenges in the offshore wind sector. Renew. Sustain. Energy Rev. 61, 141–154. http://dx.doi.org/10.1016/j.rser.2016.02.017.

Agarwala, M.K., Jamalabad, V.R., Langrana, N.A., Safari, A., Whalen, P.J., Danforth, S.C., 1996. Structural quality of parts processed by fused deposition. Rapid Prototyp. J. 2, 4–19. http://dx.doi.org/10.1108/13552549610153370.

Ahmed, A., Azam, A., Zhang, Z., Yi, M., Aslam, T., Mugheri, S.A., Hao, D., Abdelrahman, M., Tairab, A.M., 2025. An isomorphic froude scaling approach to bulbous-bottomed buoys in wave energy converters for smart floating cities. Appl. Ocean Res. 156, 104485. http://dx.doi.org/10.1016/j.apor.2025.104485, URL https://www.sciencedirect.com/science/article/pii/S0141118725000732.

Alam, M., Kim, B., Shahid, F., 2026. Flapping-foil energy harvesters: Principles, performance, and prospects. Appl. Ocean Res. 168, 104953. http://dx.doi.org/10.1016/j.apor.2026.104953, URL https://www.sciencedirect.com/science/article/pii/S0141118726000362.

Alsaadi, M., Flanagan, T., Devine, D.M., 2025. Seawater ageing effects on the mechanical performance of basalt fibre-reinforced thermoplastic and epoxy composites. J. Compos. Sci. 9, 368. http://dx.doi.org/10.3390/jcs9070368.

Aravind, A., Jerome, S., Kumar, R., 2025. Evaluation on Mechanical and Metallurgical Properties of Wire Arc Additive Manufactured ER 2209 Duplex Stainless Steel for Automotive and Marine Applications. SAE Technical Paper 2025-28-0108, SAE International, http://dx.doi.org/10.4271/2025-28-0108.

Armanfar, A., Alper Tasmektepligil, A., Kilic, R.T., Demir, S., Cam, S., Karafi, Y., Majd, B.A.E., Gunpinar, E., 2024. Embedding lattice structures into ship hulls for structural optimization and additive manufacturing. Ocean Eng. 301, 117601. http://dx.doi.org/10.1016/j.oceaneng.2024.117601, URL www.sciencedirect.com/...S0029801824009387.

Babarit, A., 2015. A database of capture width ratio of wave energy converters. Ren. Energy 80, 610–628. http://dx.doi.org/10.1016/j.renene.2015.02.049.

Balestrino, F., Coiro, D.P., Giannini, G., Giudice, D., Troise, G., 2019. Resource Assessment for the GEMSTAR Tidal Current Energy Harvester Deployment in the Strait of Messina. Naples, Italy.

Balidas, A., Kerbrat, O., Hascoet, J.Y., 2024. The potential of additive manufacturing of metal components to reduce environmental impacts. J. Mach. Eng. 24, 94–104. http://dx.doi.org/10.36897/jme/186988.

Bas-Bolufer, J., Castelló-Pedrero, P., García-Gascón, C., García-Manrique, J.A., 2025. Study and characterization of recycled ABS-GF in large format additive manufacturing to enhance mechanical properties of printed structures. Mater. Des. 259, 114707. http://dx.doi.org/10.1016/j.matdes.2025.114707.

Bekker, A.C.M., Verlinden, J.C., 2018. Life cycle assessment of wire + arc additive manufacturing compared to green sand casting and CNC milling in stainless steel. J. Clean. Prod. 177, 438–447. http://dx.doi.org/10.1016/j.jclepro.2017.12.148, URL www.sciencedirect.com/...S0959652617331074.

Belvisi, F., Piccioni, M., Ratti, A., 2024. Combining lightness and stiffness through composite-reinforced additive manufacturing in the yacht industry: Case study analysis and application on large functional components. J. Mar. Sci. Eng. 12, 918. http://dx.doi.org/10.3390/jmse12060918, URL https://www.mdpi.com/2077-1312/12/6/918, number: 6 Publisher: Multidisciplinary Digital Publishing Institute.

Bir, G.S., Lawson, M.J., Li, Y., 2011. Structural design of a horizontal-axis tidal current turbine composite blade. In: Volume 5: Ocean Space Utilization; Ocean Renewable Energy. ASMEDC, Rotterdam, The Netherlands, pp. 797–808. http://dx.doi.org/10.1115/OMAE2011-50063, URL https://asmedigitalcollection.asme.org/.../OMAE2011.

Branker, K., Pathak, M.J.M., Pearce, J.M., 2011. A review of solar photovoltaic levelized cost of electricity. Renew. Sustain. Energy Rev. 15, 4470–4482. http://dx.doi.org/10.1016/j.rser.2011.07.104, URL https://www.sciencedirect.com/.../S1364032111003492.

Cao, L., Li, J., Zhang, L., Luo, S., Li, M., Huang, X., 2023. Cross-attention-based multi-sensing signals fusion for penetration state monitoring during laser welding of aluminum alloy. Knowl.-Based Syst. 261, 110212. http://dx.doi.org/10.1016/j.knosys.2022.110212.

Caracol AM, 2026. Caracol AM — Large scale additive manufacturing. URL https://caracol-am.com/, company website.

Carallo, G.A., Casa, M., Kelly, C., Alsaadi, M., 2025. Comparative life cycle assessment (lca) of traditional and new sustainable wind blade construction. Sustainability 17, 2026. http://dx.doi.org/10.3390/su17052026.

Caron, O., Terracina, S., Faivre, L., Santicchia, A., Lefevre, F., Arcangeletti, G., 2025. Wire arc additive manufacturing (waam) component with integrated substrate for subsea tee branch application. In: Offshore Technology Conference. OnePetro, http://dx.doi.org/10.4043/35610-MS.

CEAD Group, 2024. Revolutionizing trimming fixture production with large format additive manufacturing (LFAM) technology. URL https://ceadgroup.com/resources/case-studies/revolutionizing-trimming-fixture-production-with-large-format-additive-manufacturing/. (Accessed 27 March 2026).

Chakrabarti, S.K., 2005. Handbook of Offshore Engineering, vol. II, Elsevier.

Chakraborty, D., Reddy, B.A., Choudhury, A.R., 2008. Extruder path generation for curved layer fused deposition modeling. Computer-Aided Des. 40, 235–243. http://dx.doi.org/10.1016/j.cad.2007.10.014.

Chen, Z., Han, C., Gao, M., Kandukuri, S.Y., Zhou, K., 2022. A review on qualification and certification for metal additive manufacturing. Virtual Phys. Prototyp. 17, 382–405. http://dx.doi.org/10.1080/17452759.2021.2018938.

Chen, H., Pilla, S., Li, G., Ijeoma, M.W., Carbajales-Dale, M., 2024. Electricity use in big area additive manufacturing of fiber-reinforced polymer composites. Sci. Data 11, 1362. http://dx.doi.org/10.1038/s41597-024-04240-w, URL https://www.nature.com/articles/s41597-024-04240-w, publisher: Nature Publishing Group.

Cheng, G., Li, H., Dai, H., Gao, H., Pang, J., 2023. Investigation of high-cycle fatigue properties of wire arc additive manufacturing 13cr4ni martensitic stainless steel. Metals 13, 1210. http://dx.doi.org/10.3390/met13071210.

Chivate, A., Zhou, C., 2024. Additive manufacturing of micropatterned functional surfaces: a review. Int. J. Extrem. Manuf. 6, http://dx.doi.org/10.1088/2631-7990/ad4240.

Choi, H., Adamczyk, J.M., Hernandez-Sanchez, B.A., Koss, E.K., Noell, P., Spiak, S.R., Pucket, R.V., Escarcega-Herrera, K., Love, A.S., Karasz, E., Neary, V.S., Melia, M.A., Heiden, M.J., 2024. Wire arc additive manufactured a36 steel performance for marine renewable energy systems. Int. J. Adv. Manuf. Technol. 132, 4677–4688. http://dx.doi.org/10.1007/s00170-024-13585-w.

Chu, Y.W., Wang, C.M., Ueng, T.S., Chen, J.C., 2023. Offshore fish farms: A review of standards and guidelines for design and analysis. J. Mar. Sci. Eng. 11, 762. http://dx.doi.org/10.3390/jmse11040762.

Clarke, J.A., Connor, G., Grant, A.D., Johnstone, C.M., 2007. Design and testing of a contra-rotating tidal current turbine. Proc. Inst. Mech. Eng. Part A: J. Power Energy 221, 171–179. http://dx.doi.org/10.1243/09576509JPE296.

Clemente, D., Rosa-Santos, P., Ferradosa, T., Taveira-Pinto, F., 2023. Wave energy conversion energizing offshore aquaculture: Prospects along the Portuguese coastline. Renew. Energy 204, 347–358. http://dx.doi.org/10.1016/j.renene.2023.01.009, URL https://www.sciencedirect.com/.../S0960148123000095.

co legislators, E., 1994. Directive 94/25/EC of the European Parliament and of the Council of 16 June 1994 on the approximation of the laws, regulations and administrative provisions of the Member States relating to recreational craft. Off. J. Eur. Communities L 164, 15–38, URL http://data.europa.eu/eli/dir/1994/25/oj.

Coiro, D.P., Troise, G., Scherillo, F., De Marco, A., Calise, G., Bizzarrini, N., 2017. Development, deployment and experimental test on the novel tethered system GEM for tidal current energy exploitation. Renew. Energy 114, 323–336. http://dx.doi.org/10.1016/j.renene.2017.01.040.

Crump, S.S., 1992. Apparatus and method for creating three-dimensional objects. Filed in 1989.

Dahat, S., Hurtig, K., Andersson, J., Scotti, A., 2020. A methodology to parameterize wire + arc additive manufacturing: A case study for wall quality analysis. J. Manuf. Mater. Process. 4, 14. http://dx.doi.org/10.3390/jmmp4010014.

Damen Shipyards Group, 2017. First class approved 3d printed ship's propeller, the waampeller, is unveiled. Press Release, URL https://www.damen.com/insights-and-innovation/news/first-class-approved-3d-printed-ships-propeller-the-waampeller-is-unveiled.

De Maio, A., Cozzarolo, L., Galbiati, R., et al., 2023. Effect of metal additive manufacturing surface roughness on laminar, transitional and turbulent flows. Rapid Prototyp. J. 29, 124–138. http://dx.doi.org/10.1108/RPJ-08-2022-0278.

Demirel, Y.K., Turan, O., Incecik, A., 2017. Predicting the effect of biofouling on ship resistance using cfd. Appl. Ocean Res. 62, 100–118. http://dx.doi.org/10.1016/j.apor.2016.12.003.

Dharmadhikari, S., Menon, N., Basak, A., 2023. A reinforcement learning approach for process parameter optimization in additive manufacturing. Addit. Manuf. 71, 103556. http://dx.doi.org/10.1016/j.addma.2023.103556.

Dias, M., Ribeiro, I., Silva, C.M.A., Pragana, J., Priarone, P.C., 2022. Economic and environmental potential of wire-arc additive manufacturing. Sustainability 14, 5197. http://dx.doi.org/10.3390/su14095197.

Díaz, H., Guedes Soares, C., 2020. Review of the current status, technology and future trends of offshore wind farms. Ocean Eng. 209, 107381. http://dx.doi.org/10.1016/j.oceaneng.2020.107381, URL https://www.sciencedirect.com/.../S002980182030411X.

Du Plessis, A., Yadroitsev, I., Yadroitsava, I., Le Roux, S.G., 2018. X-ray microcomputed tomography in additive manufacturing: A review of the current technology and applications. 3D Print. Addit. Manuf. 5, 227–247. http://dx.doi.org/10.1089/3dp.2018.0060.

Duty, C.E., Kunc, V., Compton, B., Post, B., Erdman, D., Smith, R., Lind, R., Lloyd, P., Love, L., 2017. Structure and mechanical behavior of big area additive manufacturing (baam) materials. Rapid Prototyp. J. 23, 181–189. http://dx.doi.org/10.1108/RPJ-12-2015-0183.

Ermakova, A., Ganguly, S., Razavi, J., Berto, F., 2022. Corrosion-fatigue crack growth behaviour of wire arc additively manufactured er70s-6 steel parts in marine environments. Eur. J. Mech. A Solids 96, 104739. http://dx.doi.org/10.1016/j.euromechsol.2022.104739.

European Commission, 2025. Climate action - european commission. URL https://climate.ec.europa.eu/index_en. (Accessed 17 September 2025).

Falcão, A.F.d.O., 2010. Wave energy utilization: A review of the technologies. Ren. Sustain. Energy Rev. http://dx.doi.org/10.1016/j.rser.2009.11.003.

Fang, Y., Kim, M.K., Zhang, Y., Kim, T., No, J., Suhr, J., 2023. A new grain refinement route for duplex stainless steels: Micro-duplex stainless steel matrix composites processed by laser powder bed fusion. Mater. Sci. Eng.: A 881, 145351. http://dx.doi.org/10.1016/j.msea.2023.145351, URL https://www.sciencedirect.com/.../S092150932300775X.

Feier, A., Buta, I., Florica, C., Blaga, L., 2023. Optimization of wire arc additive manufacturing (WAAM) process for the production of mechanical components using a CNC machine. Materials 16, 17. http://dx.doi.org/10.3390/ma16010017, URL https://www.mdpi.com/1996-1944/16/1/17, number: 1 Publisher: Multidisciplinary Digital Publishing Institute.

Fernández, E., Ayas, C., Langelaar, M., Duysinx, P., 2021. Topology optimisation for large-scale additive manufacturing: generating designs tailored to the deposition nozzle size. Virtual Phys. Prototyp. 16, 196–220. http://dx.doi.org/10.1080/17452759.2021.1914893.

Flack, K.A., Schultz, M.P., 2014. Roughness effects on wall-bounded turbulent flows. Phys. Fluids 26, 101305. http://dx.doi.org/10.1063/1.4896280.

Franke, J., Heinrich, F., Reisch, R.T., 2025. Vision based process monitoring in wire arc additive manufacturing (waam). J. Intell. Manuf. 36, 1711–1721. http://dx.doi.org/10.1007/s10845-023-02287-x.

Gao, Q., Ertugrul, N., Ding, B., Negnevitsky, M., 2020. Offshore wind, wave and integrated energy conversion systems: A review and future. pp. 1–6.

Garg, H., Wang, L., Fureby, C., 2024. Heat transfer enhancement with additively manufactured rough surfaces: Insights from large-eddy simulations. Phys. Fluids 36, http://dx.doi.org/10.1063/5.0189115.

Garofalo, J., Shah, R., Thomas, G., Shirvani, K., Marian, M., Rosenkranz, A., 2024. Additive manufacturing in the maritime industry: A perspective on current trends and future needs. J. Ship Prod. Des. 40, 36–43. http://dx.doi.org/10.5957/JSPD.05230005.

Gerwick, B.C., 2007. Construction of Marine and Offshore Structures, third ed. CRC Press, Boca Raton, http://dx.doi.org/10.1201/9780849330520.

Giannini, G., Day, S., Rosa-Santos, P., Taveira-Pinto, F., 2021a. A novel 2-D point absorber numerical modelling method. Inventions 6, 75.

Giannini, G., Giorgi, G., Rosa-Santos, P., Taveira-Pinto, F., Mattiazzo, G., Ramos, V., Giorcelli, E., 2025. Multi-objective development of a point absorber wave energy converter using dynamic modelling. In: Proceedings of the European Wave and Tidal Energy Conference, vol. 16, http://dx.doi.org/10.36688/ewtec-2025-1128, URL https://publications.evolvingcities.org/.../1128.

Giannini, G., López, M., Ramos, V., Rodríguez, C., Rosa-Santos, P., Taveira-Pinto, F., 2021b. Geometry assessment of a sloped type wave energy converter. Renew. Energy 171, 672–686. http://dx.doi.org/10.1016/j.renene.2021.02.132.

Giannini, G., Rosa-Santos, P., Ramos, V., Taveira-Pinto, F., 2020a. On the development of an offshore version of the CECO wave energy converter. Energies 13, http://dx.doi.org/10.3390/en13051036.

Giannini, G., Rosa-Santos, P., Ramos, V., Taveira-Pinto, F., 2022. Wave energy converters design combining hydrodynamic performance and structural assessment. Energy.

Giannini, G., Temiz, I., Rosa-Santos, P., Shahroozi, Z., Ramos, V., Göteman, M., Engström, J., Day, S., Taveira-Pinto, F., 2020b. Wave energy converter power take-off system scaling and physical modelling. J. Mar. Sci. Eng. 8, 632.

Giannini, G., Zavvar, E., Ramos, V., Calheiros-Cabral, T., Iglesias, I., Taveira-Pinto, F., Rosa-Santos, P., 2024. On the development of a near-shore pivoting wave energy converter. Energies 17, http://dx.doi.org/10.3390/en17112695.

Goh, G.D., Kin Keong, W., Nigel, T., Hang Li, S., Nai, M.L.S., 2024. Large-format additive manufacturing of polymers: a review of fabrication processes, materials, and design. Virtual Phys. Prototyp. 19, e2336160. http://dx.doi.org/10.1080/17452759.2024.2336160, publisher: Taylor & Francis _eprint.

Gonçalves, R.M., Martinho, A., Oliveira, J.P., 2022. Recycling of reinforced glass fibers waste: Current status. Materials 15, 1596. http://dx.doi.org/10.3390/ma15041596, URL https://www.mdpi.com/1996-1944/15/4/1596, number: 4 Publisher: Multidisciplinary Digital Publishing Institute.

Gonzales, M.A.C., Kujala, P., 2021. Additive manufacturing of miniature marine structures for crashworthiness verification: A numerical revision. Appl. Ocean Res. 111, 102653. http://dx.doi.org/10.1016/j.apor.2021.102653, URL https://www.sciencedirect.com/.../S0141118721001309.

Greer, C., Nycz, A., Noakes, M., Richardson, B., Post, B., Kurfess, T., Love, L., 2019. Introduction to the design rules for metal big area additive manufacturing. Addit. Manuf. 27, 159–166. http://dx.doi.org/10.1016/j.addma.2019.02.016, URL www.sciencedirect.com/...S2214860418309345.

He, T., Yu, S., Shi, Y., Huang, A., 2020. Forming and mechanical properties of wire arc additive manufacture for marine propeller bracket. J. Manuf. Process. 52, 96–105. http://dx.doi.org/10.1016/j.jmapro.2020.01.053.

Henao, Y., Nicholson, C., Huff, J., Korey, M., Gentry, R., Ozcan, S., 2023. Wind turbine blade repurposing and recycling: Coupling repurposing methods with 3d printing technology. In: Proceedings of the International Conference on Non-Conventional Materials and Technologies. NOCMAT, URL https://static.even3.com/anais/663734.pdf, oSTI ID: 2311242.

Honarvar, F., Varvani-Farahani, A., 2020. A review of ultrasonic testing applications in additive manufacturing: Defect evaluation, material characterization, and process control. Ultrasonics 108, 106227. http://dx.doi.org/10.1016/j.ultras.2020.106227, URL www.sciencedirect.com/...S0041624X20301669.

Hu, Y., Jiang, X., Huo, G., Su, C., Li, H., Zheng, Z., 2022. A novel adaptive slicing algorithm based on ameliorative area ratio and accurate cusp height for 3d printing. Rapid Prototyp. J. 28, 453–465. http://dx.doi.org/10.1108/RPJ-12-2020-0319.

Huang, Y., Leu, M.C., Mazumder, J., Donmez, A., 2015. Additive Manufacturing: Current state, future potential, gaps and needs, and recommendations. J. Manuf. Sci. Eng. 137, http://dx.doi.org/10.1115/1.4028725.

Hull, C.W., 1986. Apparatus for production of three-dimensional objects by stereolithography.

Ibrahim, M., Hulme, C., Grasmo, G., Aune, R.E., 2024. Preliminary evaluation of nickel silicide (NiSi12-wt%) laser cladding for enhancing microhardness and corrosion resistance of S355 steel. Metals 14, 1389. http://dx.doi.org/10.3390/met14121389, URL https://www.mdpi.com/2075-4701/14/12/1389, number: 12 Publisher: Multidisciplinary Digital Publishing Institute.

ISO Org., 2020. ISO 21062:2020: Corrosion of metals and alloys — Determination of the corrosion rates of embedded steel reinforcement in concrete exposed to simulated marine environments.

Jones, R., Haufe, P., Sells, E., Iravani, P., Olliver, V., Palmer, C., Bowyer, A., 2011. Reprap–the replicating rapid prototyper. Robotica 29, 177–191. http://dx.doi.org/10.1017/S026357471000069X.

Junghans, E., Govindaraj, R.B., Andersen, I., Worm, N., 2020. Certification of additively manufactured materials for maritime application. Mater. Des. Process. Commun. 2, e144. http://dx.doi.org/10.1002/mdp2.144.

Karimi, S., Kwon, S., Ning, F., 2021. Energy-aware production scheduling for additive manufacturing. J. Clean. Prod. 278, 123183. http://dx.doi.org/10.1016/j.jclepro.2020.123183.

Karunanithi, S., Arasappan, R.K., Nallathambi, S.S., 2026. Effect of heat treatment temperature on the phase composition, mechanical properties and corrosion resistance of wire arc additive manufactured duplex stainless steel. Rapid Prototyp. J. 32, 162–179. http://dx.doi.org/10.1108/RPJ-03-2025-0116.

Kasperovich, G., Hausmann, J., 2015. Improvement of fatigue resistance and ductility of tial6v4 processed by selective laser melting. J. Mater. Process. Technol. 220, 202–214. http://dx.doi.org/10.1016/j.jmatprotec.2015.01.025.

Keeley, N., Pochon, X., Wood, S.A., Laroche, O., Zaiko, A., 2021. Comparison of biofouling on 3d-printing materials in the marine environment. Int. Biodeterior. Biodegrad. 164, 105293. http://dx.doi.org/10.1016/j.ibiod.2021.105293.

Keshavarzan, M., Mohammadi, M., 2024. A comprehensive metal additive manufacturing platform to transform the marine industry. MATEC Web Conf. 401, 02013. http://dx.doi.org/10.1051/matecconf/202440102013, URL https://www.matec-conferences.org/.../202440102013.

Khajavi, A.R., Andersen, R.B., Wan-Wendner, R., 2021. Wire arc additive manufacturing for repairing aluminium structures in marine applications. Mater. Lett. 299, 130112. http://dx.doi.org/10.1016/j.matlet.2021.130112.

Khoshnevis, B., 2004. Automated construction by contour crafting—related robotics and information technologies. Autom. Constr. 13, 5–19. http://dx.doi.org/10.1016/j.autcon.2003.08.012.

Kofoed, J.P., Folley, M., 2016. Chapter 13 - Determining mean annual energy production. In: Folley, M. (Ed.), Numerical Modelling of Wave Energy Converters. Academic Press, pp. 253–266. http://dx.doi.org/10.1016/B978-0-12-803210-7.00013-X, URL www.sciencedirect.com/...B978012803210700013X.

Kok, Y., Tan, X.P., Wang, P., Nai, M.L.S., Loh, N.H., Liu, E., Tor, S.B., 2018. Anisotropy of additively manufactured metallic materials: A review. Virtual Phys. Prototyp. 13, 255–284. http://dx.doi.org/10.1080/17452759.2017.1396953.

Korey, M., Hubbard, A.M., Haye, G., Bedsole, R., Skelton, Z., Meshkat, N., Anilal, A.L.S., Slavny, K., Copenhaver, K., Corum, T., Bones, D.X., Gramlich, W.M., Duty, C., Ozcan, S., 2025. Enabling industrial re-use of large-format additive manufacturing molding and tooling. Polymers 17, 2981. http://dx.doi.org/10.3390/polym17222981.

Kostidi, E., Nikitakos, N., 2024. Revolutionizing the marine spare parts supply chain through additive manufacturing: A system dynamics simulation case study. J. Mar. Sci. Eng. 12, 1515. http://dx.doi.org/10.3390/jmse12091515.

Kumar, N., Ukey, P.D., Francis, V., Singh, R.P., Sahu, S., 2022. Chapter 16 - Plastic pellets. In: Izdebska-Podsiadły, J. (Ed.), Polymers for 3D Printing. William Andrew Publishing Plastics Design Library, pp. 307–323. http://dx.doi.org/10.1016/B978-0-12-818311-3.00019-7, URL www.sciencedirect.com/...B9780128183113000197.

Lampros, E., Zervaki, A.D., 2026. Maritime applications as motivation for analytical calculation of thermal history in low-carbon mild steel waam cylinders. Metals 16, 192. http://dx.doi.org/10.3390/met16020192.

Le Méhauté, B., 1969. An Introduction to Hydrodynamics and Water Waves. Springer, Berlin, Heidelberg.

Lehmann, T., Rose, D., Ranjbar, E., Ghasri-Khouzani, M., Tavakoli, M., Henein, H., Wolfe, T., Jawad Qureshi, A., 2022. Large-scale metal additive manufacturing: a holistic review of the state of the art and challenges. Int. Mater. Rev. 67, 410–459. http://dx.doi.org/10.1080/09506608.2021.1971427.

Li, J., Wang, G., Li, Z., Yang, S., Chong, W.T., Xiang, X., 2020. A review on development of offshore wind energy conversion system. Int. J. Energy Res. 44, 9283–9297. http://dx.doi.org/10.1002/er.5751, URL.

Liu, Y., Ren, H., Zhang, Q., Yuan, P., Ma, H., Li, Y., Zhang, Y., Ning, J., 2026. Monitoring and control of the direct energy deposition (ded) additive manufacturing process using deep learning techniques: A review. Materials 19, 89. http://dx.doi.org/10.3390/ma19010089.

Lotwala, T., Schoop, J., Khanna, N., 2025. Life cycle assessment to achieve sustainability in pre- and post-processing: Waam vs. wrought ti-6al-4v. In: Proceedings of the ASME 2025 International Mechanical Engineering Congress and Exposition (IMECE-INDIA). http://dx.doi.org/10.1115/IMECE-INDIA2025-160694, V001T01A027.

Love, A., Behseresht, S., Park, Y.H., 2025. Reinforcement learning enabled intelligent process monitoring and control of wire arc additive manufacturing. J. Manuf. Mater. Process. 9, 340. http://dx.doi.org/10.3390/jmmp9100340.

Love, L.J., Nycz, A., Noakes, M., Post, B., Babu, A.R., 2016. Development and Demonstration of Large-Scale MetalAdditive Manufacturing for Military Vehicle Applications – Final Report. Oak Ridge National Lab. (ORNL), Oak Ridge, TN (United States), http://dx.doi.org/10.2172/1240215, Final Report ORNL/TM-2017/5.

Luznik, L., Flay, R.J., Walker, J., et al., 2020. The effect of surface roughness on the hydrodynamic performance of 3D printed hydrofoils. Ocean Eng. 202, 107142. http://dx.doi.org/10.1016/j.oceaneng.2020.107142.

Mancuso, A., Saporito, A., Tumino, D., 2022. Designing the internal reinforcements of a sailing boat using a topology optimization approach. Appl. Ocean Res. 129, 103384. http://dx.doi.org/10.1016/j.apor.2022.103384, URL www.sciencedirect.com/...S0141118722003157.

Manford, D., Budinoff, H.D., Bushra, J., 2022. Accuracy of build time and mass estimates from slicer software for fused filament fabrication. Manuf. Lett. 33, 752–757. http://dx.doi.org/10.1016/j.mfglet.2022.07.092, URL www.sciencedirect.com/...S2213846322001237.

Manolache, A.I., Andrei, G., 2024. A comprehensive review of multi-use platforms for renewable energy and aquaculture integration. Energies 17, 4816. http://dx.doi.org/10.3390/en17194816, URL https://www.mdpi.com/1996-1073/17/19/4816, number: 19 Publisher: Multidisciplinary Digital Publishing Institute.

Marqués, A., Dieste, J.A., Monzón, I., Laguía, A., Javierre, C., Elduque, D., 2024. Analysis of energy and material consumption for the manufacturing of an aeronautical tooling: An experimental comparison between pure machining and big area additive manufacturing. Materials 17, 3066. http://dx.doi.org/10.3390/ma17133066, URL https://www.mdpi.com/1996-1944/17/13/3066, publisher: Multidisciplinary Digital Publishing Institute.

Materialise, 2020. 30 years of innovation: How stereolithography sparked materialise's inventive ethos. Materialise Technical Archive, Leuven, Belgium.

Miranda, F., Rosa-Santos, P., Taveira-Pinto, F., Guan, D., Fazeres-Ferradosa, T., 2025. Aquaculture and offshore wind: A review of co-location design challenges. Ocean Eng. 318, 120161. http://dx.doi.org/10.1016/j.oceaneng.2024.120161.

Moreno Nieto, D., Alonso-García, M., Pardo-Vicente, M.A., Rodríguez-Parada, L., 2021. Product design by additive manufacturing for water environments: Study of degradation and absorption behavior of PLA and PETG. Polymers 13, 1036. http://dx.doi.org/10.3390/polym13071036, URL https://www.mdpi.com/2073-4360/13/7/1036, number: 7 Publisher: Multidisciplinary Digital Publishing Institute.

Moreno Nieto, D., Casal López, V., Molina, S.I., 2018. Large-format polymeric pellet-based additive manufacturing for the naval industry. Addit. Manuf. 23, 79–85. http://dx.doi.org/10.1016/j.addma.2018.07.012, URL www.sciencedirect.com/...S2214860418301726.

Moreno Nieto, D., Molina, S.I., 2020. Large-format fused deposition additive manufacturing: a review. Rapid Prototyp. J. 26, 793–799. http://dx.doi.org/10.1108/RPJ-05-2018-0126.

Morthorst, P., Kitzing, L., 2016. 2 - economics of building and operating offshore wind farms. In: Ng, C., Ran, L. (Eds.), Offshore Wind Farms. Woodhead Publishing, pp. 9–27. http://dx.doi.org/10.1016/B978-0-08-100779-2.00002-7, URL www.sciencedirect.com/...B9780081007792000027.

Murdy, P., Candon, C., Samborsky, D., Miller, D., Beach, R., 2024. Polymer additive manufacturing for marine renewable energy applications: Best practices, research trends, and current challenges. http://dx.doi.org/10.2172/2447830, URL.

Murdy, P., Dolson, J., Miller, D., Hughes, S., Beach, R., 2021. Leveraging the advantages of additive manufacturing to produce advanced hybrid composite structures for marine energy systems. Appl. Sci. 11, 1336. http://dx.doi.org/10.3390/app11031336, URL https://www.mdpi.com/2076-3417/11/3/1336, number: 3 Publisher: Multidisciplinary Digital Publishing Institute.

Muryadin, Muttaqie, T., Sasmito, C., Noor, F.M., Nugroho, A.C.P.T., Priatno, D.H., Hakim, B.A., Fuadi, A.P., Khoirudin, M.H., Wibowo, T., Putra, A.M.F., 2023. Dynamic response of high-speed craft bottom panels subjected to slamming loadings. URL https://www.degruyterbrill.com/document/doi/10.1515/, section: Curved and Layered Structures.

Nguyen, H.T., Safder, U., Nhu Nguyen, X.Q., Yoo, C., 2020. Multi-objective decision-making and optimal sizing of a hybrid renewable energy system to meet the dynamic energy demands of a wastewater treatment plant. Energy 191, 116570. http://dx.doi.org/10.1016/j.energy.2019.116570, URL www.sciencedirect.com/...S0360544219322650.

Nieto, D.M., Molina, S.I., 2020. Large-format fused deposition additive manufacturing: a review. Rapid Prototyp. J. 26, 793–799. http://dx.doi.org/10.1108/RPJ-05-2018-0126, URL https://www.emerald.com/insight/content/doi/10.1108, publisher: Emerald Publishing Limited.

Okushemiya, D., Rusch, C.J., Robertson, B., Zhang, Z., 2026. Model validation and improved pto modeling of a field-deployed wave energy converter with tethered heave plate. Appl. Ocean Res. 166, 104921. http://dx.doi.org/10.1016/j.apor.2026.104921, URL https://www.sciencedirect.com/science/article/pii/S0141118726000052.

O'Neill, F., Mehmanparast, A., 2024. A review of additive manufacturing capabilities for potential application in offshore renewable energy structures. Forces Mech. 14, 100255. http://dx.doi.org/10.1016/j.finmec.2024.100255, URL www.sciencedirect.com/...S2666359724000015.

Orszaghova, J., Rafiee, A., Wolgamot, H., Draper, S., Taylor, P.H., 2016. Experimental study of extreme responses of a point absorber wave energy converter.

Palm, J., Eskilsson, C., Paredes, G., Bergdahl, L., 2018. Assessment of scale effects, viscous forces and induced drag on a point-absorbing wave energy converter by CFD simulations. J. Mar. Sci. Eng. 6, 124. http://dx.doi.org/10.3390/jmse6040124.

Pan, J., Lin, Y., Hong, J., He, F., 2025. Experimental investigation of the breakwater consisting of an array of cylindrical oscillating water column devices: Hydrodynamic characteristics and wave energy conversion. Appl. Ocean Res. 158, 104520. http://dx.doi.org/10.1016/j.apor.2025.104520, URL https://www.sciencedirect.com/science/article/pii/S0141118725001087.

Parmeggiani, S., Kofoed, J.P., Friis-Madsen, E., 2011. Extreme loads on the mooring lines and survivability mode for the wave dragon wave energy converter. pp. 2159–2166.

Pegues, J., Roach, M., Williamson, R., Shamsaei, N., 2018. Surface roughness effects on the fatigue strength of additively manufactured ti-6al-4v. Int. J. Fatigue 116, 543–552. http://dx.doi.org/10.1016/j.ijfatigue.2018.07.013.

Peterson, E., 2022. Recent innovations in additive manufacturing for marine vessels. Marit. Technol. Res. 4, http://dx.doi.org/10.33175/mtr.2022.257491, 257491–257491, URL https://so04.tci-thaijo.org/index.php/MTR/article/view/257491, number: 4.

Pignatelli, F., Percoco, G., 2022. An application- and market-oriented review on large format additive manufacturing, focusing on polymer pellet-based 3D printing. Prog. Addit. Manuf. 7, 1363–1377. http://dx.doi.org/10.1007/s40964-022-00309-3.

Pinho, A.C., Piedade, A.P., 2025. Additive manufacturing of TPU/C and PVDF/graphene composites with adjustable mechanical and conductive properties for sensor applications. Results Eng. 27, 105760. http://dx.doi.org/10.1016/j.rineng.2025.105760, URL www.sciencedirect.com/...S2590123025018316.

Post, N., Cairns, J., Skelton, J., Pisani, W., Kimball, J., Van Rij, J., Brenna, R., O'Connor, P., 2021. Leveraging the advantages of additive manufacturing to produce advanced hybrid composite structures for marine energy systems. Appl. Sci. 11, 1336. http://dx.doi.org/10.3390/app11031336.

Ramos, V., Giannini, G., Calheiros-Cabral, T., López, M., Rosa-Santos, P., Taveira-Pinto, F., 2022. Assessing the effectiveness of a novel WEC concept as a co-located solution for offshore wind farms. J. Mar. Sci. Eng. 10, 267.

Ramos, V., Giannini, G., Calheiros-Cabral, T., Rosa-Santos, P., Taveira-Pinto, F., 2021. Legal framework of marine renewable energy: A review for the Atlantic region of Europe. Renew. Sustain. Energy Rev. 137, 110608. http://dx.doi.org/10.1016/j.rser.2020.110608.

Ramsay, W., Goupee, A., Allen, C., Viselli, A., Kimball, R., 2022. Optimization of a lightweight floating offshore wind turbine with water ballast motion mitigation technology. Wind 2, 535–570. http://dx.doi.org/10.3390/wind2030029, URL https://www.mdpi.com/2674-032X/2/3/29, number: 3 Publisher: Multidisciplinary Digital Publishing Institute.

Ribeiro, A., Murphy, J., Norrish, J., 1996. The way forward for shaped metal deposition. Weld. Met. Fabr. 64, 14–18.

Roga, S., Bardhan, S., Kumar, Y., Dubey, S.K., 2022. Recent technology and challenges of wind energy generation: A review. Sustain. Energy Technol. Assess. 52, 102239. http://dx.doi.org/10.1016/j.seta.2022.102239, URL www.sciencedirect.com/...S2213138822002910.

Romani, A., Paramatti, M., Gallo, L., Levi, M., 2024. Large-format material extrusion additive manufacturing of pla, ldpe, and hdpe compound feedstock with spent coffee grounds. Int. J. Adv. Manuf. Technol. 134, 1845–1861. http://dx.doi.org/10.1007/s00170-024-14214-2.

Roseman, M., Martin, R., Morgan, G., 2016. 10 - Composites in offshore oil and gas applications. In: Graham-Jones, J., Summerscales, J. (Eds.), Marine Applications of Advanced Fibre-Reinforced Composites. In: Woodhead Publishing Series in Composites Science and Engineering, Woodhead Publishing, pp. 233–257. http://dx.doi.org/10.1016/B978-1-78242-250-1.00010-7, URL www.sciencedirect.com/...B9781782422501000107.

Roshan, M., Mahtabi, M., Bednarczyk, W., Cios, G., Haghshenas, M., 2026. Effect of pre-corrosion on the fatigue performance of direct energy deposited nickel–aluminum bronze. Mater. Chem. Phys. 349, 131759. http://dx.doi.org/10.1016/j.matchemphys.2025.131759.

Rubino, F., Nisticò, A., Tucci, F., Carlone, P., 2020. Marine application of fiber reinforced composites: A review. J. Mar. Sci. Eng. 8, 26. http://dx.doi.org/10.3390/jmse8010026, URL https://www.mdpi.com/2077-1312/8/1/26, number: 1 Publisher: Multidisciplinary Digital Publishing Institute.

Sabic, C., 2022. Enabling growth for pellet-fed additive manufacturing. URL https://materialfinder.sabic-specialties.com.

Salar, D., Dupuis, A., Engström, J., Hultman, E., 2026. Emulating wave energy converter operation in irregular waves using a robotized dry test rig. Appl. Ocean Res. 166, 104920. http://dx.doi.org/10.1016/j.apor.2026.104920, URL https://www.sciencedirect.com/science/article/pii/S0141118726000040.

Schürmann, M., Varshneya, S., Klar, M., Ghansiyal, S., Kloft, M., Aurich, J.C., 2025. A framework for in-situ process control in metal additive manufacturing using anomaly-driven reinforcement learning. Procedia CIRP http://dx.doi.org/10.1016/j.procir.2025.03.050.

Schweizer, K., Bhandari, S., Lopez-Anido, R.A., Korey, M., Tekinalp, H., 2024. Recycling large-format 3d printed polymer composite formworks used for casting precast concrete – technical feasibility and challenges. J. Compos. Constr. http://dx.doi.org/10.1061/JCCOF2.CCENG-4758.

Shah, I.H., Hadjipantelis, N., Walter, L., Myers, R.J., Gardner, L., 2023. Environmental life cycle assessment of wire arc additively manufactured steel structural components. J. Clean. Prod. 389, 136071. http://dx.doi.org/10.1016/j.jclepro.2023.136071, URL www.sciencedirect.com/...S0959652623002299.

Shakil, S.I., Shakerin, S., Rahmdel, K., Mohammadi, M., Tridello, A., Paolino, D.S., Shao, S., Shamsaei, N., Haghshenas, M., 2024. Fatigue response of wire-arc additive manufactured nickel-aluminum bronze (NAB) in the post-annealed condition. Int. J. Fatigue 187, 108472. http://dx.doi.org/10.1016/j.ijfatigue.2024.108472.

Shenoi, R.A., Dulieu-Barton, J.M., Quinn, S., Blake, J.I.R., Boyd, S.W., 2011. Composite materials for marine applications: Key challenges for the future. In: Nicolais, L., Meo, M., Milella, E. (Eds.), Composite Materials. Springer, London, pp. 69–89. http://dx.doi.org/10.1007/978-0-85729-166-0_3.

Sirigu, A.S., Bonfanti, M., Begovic, E., Bertorello, C., Dafnakis, P., Giorgi, G., Bracco, G., Mattiazzo, G., 2020a. Experimental investigation of the mooring system of a wave energy converter in operating and extreme wave conditions. J. Mar. Sci. Eng. 8, http://dx.doi.org/10.3390/jmse8030180.

Sirigu, S.A., Foglietta, L., Giorgi, G., Bonfanti, M., Cervelli, G., Bracco, G., Mattiazzo, G., 2020b. Techno-economic optimisation for a wave energy converter via genetic algorithm. J. Mar. Sci. Eng. 8, http://dx.doi.org/10.3390/jmse8070482.

Sola, A., Trinchi, A., 2023. Recycling as a key enabler for sustainable additive manufacturing of polymer composites: A critical perspective on fused filament fabrication. Polymers 15, 4219. http://dx.doi.org/10.3390/polym15214219.

Sözen, A., Neşer, G., 2025. A critical systematic scoping review on the applications of additive manufacturing (am) in the marine industry. Polymers 17, 4. http://dx.doi.org/10.3390/polym17010004.

Spreafico, C., Kokare, S., Godina, R., 2026. Prospective life cycle assessment of future wire arc additive manufacturing deposition process for large-scale steel parts. Environ. Impact Assess. Rev. 116, 108111. http://dx.doi.org/10.1016/j.eiar.2025.108111.

Stankovic, D., Obande, W., Devine, M., Bajpai, A., Ó Brádaigh, C.M., Ray, D., 2024. Accelerated seawater ageing and fatigue performance of glass fibre reinforced thermoplastic composites for marine and tidal energy applications. Compos. Part C: Open Access 14, 100470. http://dx.doi.org/10.1016/j.jcomc.2024.100470.

Sun, L., Jiang, F., Huang, R., Yuan, D., Guo, C., Wang, J., 2020. Anisotropic mechanical properties and deformation behavior of low-carbon high-strength steel component fabricated by wire and arc additive manufacturing. Mater. Sci. Eng.: A 787, 139514. http://dx.doi.org/10.1016/j.msea.2020.139514.

Sun, C., Wang, Y., McMurtrey, M.D., Jerred, N.D., Liou, F., Li, J., 2021. Additive manufacturing for energy: A review. Appl. Energy 282, 116041. http://dx.doi.org/10.1016/j.apenergy.2020.116041.

Sword, J.I., Galloway, A., Toumpis, A., 2024. Analysis of environmental impact and mechanical properties of inconel 625 produced using wire arc additive manufacturing. Sustainability 16, 4178. http://dx.doi.org/10.3390/su16104178.

Tallon, P., Wilson, M., 2020. A holistic approach to additive manufacture; from design for AM to part verification in product development. pp. 411–417. http://dx.doi.org/10.1007/978-3-030-20216-3_38.

Vafadar, A., Guzzomi, F., Rassau, A., Hayward, K., 2021. Advances in metal additive manufacturing: A review of common processes, industrial applications, and current challenges. Appl. Sci. 11, 1213. http://dx.doi.org/10.3390/app11031213, URL https://www.mdpi.com/2076-3417/11/3/1213, number: 3 Publisher: Multidisciplinary Digital Publishing Institute.

Vanerio, D., Guagliano, M., Bagherifard, S., 2024. Emerging trends in large format additive manufacturing processes and hybrid techniques. Prog. Addit. Manuf. http://dx.doi.org/10.1007/s40964-024-00771-1.

Veiga, F., Villabona, E., Suárez, A., Rivero, P., Aldalur, E., 2026. LFAM with Metallic Materials—Applications. John Wiley & Sons, Ltd, pp. 393–438. http://dx.doi.org/10.1002/9783527844807.ch14, chapter 14, URL https://onlinelibrary.wiley.com/doi/abs/10.1002/9783527844807.ch14.

Vicente, C.M.S., Sardinha, M., Reis, L., Ribeiro, A., Leite, M., 2023. Large-format additive manufacturing of polymer extrusion-based deposition systems: review and applications. Prog. Addit. Manuf. 8, 1257–1280. http://dx.doi.org/10.1007/s40964-023-00397-9.

Volino, R.J., Schultz, M.P., Flack, K.A., 2011. Turbulence structure in boundary layers over periodic two- and three-dimensional roughness. J. Fluid Mech. 676, 172–190. http://dx.doi.org/10.1017/s0022112011000383.

Volpato, N., Kretschek, D., Foggiatto, J.A., Gomez da Silva Cruz, C.M., 2015. Experimental analysis of an extrusion system for additive manufacturing based on polymer pellets. Int. J. Adv. Manuf. Technol. 81, 1519–1531. http://dx.doi.org/10.1007/s00170-015-7300-2, URL https://link.springer.com/article/10.1007/s00170-015-7300-2, number: 9 Publisher: Springer.

Walker, J., Flack, K., Lust, E., Schultz, M., Luznik, L., 2014. Experimental and numerical studies of blade roughness and fouling on marine current turbine performance. Renew. Energy 66, 257–267. http://dx.doi.org/10.1016/j.renene.2013.12.021.

White, F.M., 2016. Fluid Mechanics, 8th ed. McGraw-Hill Education.

Wilson, J.F.e.a., 2003. Dynamics of Offshore Structures. John W. and Sons, Inc..

Wrzask, K., 2023. Vessel energy requirement prediction from acceleration stage towing tests on scale models. Pol. Marit. Res. 30, 4–10. http://dx.doi.org/10.2478/pomr-2023-0017.

Wu, B., Pan, Z., Ding, D., Cuiuri, D., Li, H., Xu, J., Norrish, J., 2018. A review of the wire arc additive manufacturing of metals: properties, defects and quality improvement. J. Manuf. Process. 35, 127–139. http://dx.doi.org/10.1016/j.jmapro.2018.08.001, URL www.sciencedirect.com/...S1526612518310739.

Xiong, J., Li, Y.J., Yin, Z.Q., Chen, H., 2018. Determination of surface roughness in wire and arc additive manufacturing based on laser vision sensing. Chin. J. Mech. Eng. 31, http://dx.doi.org/10.1186/s10033-018-0276-8.

Xu, T., Haas, K.A., Gunawan, B., 2023. Estimating annual energy production from short tidal current records. Renew. Energy 207, 105–115. http://dx.doi.org/10.1016/j.renene.2023.02.107, URL www.sciencedirect.com/...S0960148123002586.

Yalçınkaya, S., Yoldaş, D.M., Yoldaş, M.F., 2025. Experimental investigation of the effect of seawater on glass and carbon fiber composites via mechanical characterization. J. Compos. Sci. 9, 107. http://dx.doi.org/10.3390/jcs9030107.

Yang, J., Jung, Y., Jung, J., Ock, J.D., Cho, S., Park, S.H., Lee, T.H., Park, J., 2024. Optimized build orientation and laser scanning strategies for reducing thermal residual stress in topology-optimized automotive components. Metals 14, 1277. http://dx.doi.org/10.3390/met14111277, URL https://www.mdpi.com/2075-4701/14/11/1277, number: 11 Publisher: Multidisciplinary Digital Publishing Institute.

Ye, L., Xue, H., Li, Z., Zhou, Y., Chen, G., Xu, F., Melentiev, R., Newman, S., Yu, N., 2025. Review of online quality control for laser directed energy deposition (lded) additive manufacturing. Int. J. Extrem. Manuf. 7, 062005. http://dx.doi.org/10.1088/2631-7990/aded4f.

Zanuttigh, B., Pareschi, P., Dallavalle, E., Formentin, S.M., Gaeta, M.G., 2026. Physical modelling of the seabacus wave energy converter. Appl. Ocean Res. 166, 104905. http://dx.doi.org/10.1016/j.apor.2025.104905, URL https://www.sciencedirect.com/science/article/pii/S0141118725004900.

Zeng, Q., Thill, C., Hekkenberg, R., Rotteveel, E., Hopman, H., 2019. A modification of the ITTC57 correlation line for shallow water. J. Mar. Sci. Technol. 24, 642–657. http://dx.doi.org/10.1007/s00773-018-0578-7.

Zhang, X., Li, M., Lim, J.H., Weng, Y., Tay, Y.W.D., Pham, H., Pham, Q.C., 2018. Large-scale 3d printing by a team of mobile robots. Autom. Constr. 95, 98–106. http://dx.doi.org/10.1016/j.autcon.2018.08.004.

Zhang, H., Li, R., Liu, J., Wang, K., Weijian, Q., Shi, L., Lei, L., He, W., Wu, S., 2024. State-of-art review on the process-structure-properties-performance linkage in wire arc additive manufacturing. Virtual Phys. Prototyp. 19, e2390495. http://dx.doi.org/10.1080/17452759.2024.2390495.

Zhang, G., Wang, Y., Chen, Z., Xu, X., Dong, K., Xiong, Y., 2023. Robot-assisted conformal additive manufacturing for continuous fibre-reinforced grid-stiffened shell structures. Virtual Phys. Prototyp. 18, http://dx.doi.org/10.1080/17452759.2023.2203695.

Zheng, Y., Le, Q.T., Dao, M.H., Magee, A.R., 2019. Optimization of honeycomb shape for mitigation of flow deficit behind a separation wall. Appl. Ocean Res. 91, 101869. http://dx.doi.org/10.1016/j.apor.2019.101869, URL www.sciencedirect.com/...S0141118718308721.

Zhu, Y., Abali, B.E., Völlmecke, C., 2026. Explainable ai analysis of printing parameter effects on life cycle assessment for sustainable material-extrusion additive manufacturing. Virtual Phys. Prototyp. http://dx.doi.org/10.1080/17452759.2026.2632456.

Ziółkowski, M., Dyl, T., 2020. Possible applications of additive manufacturing technologies in shipbuilding: A review. Machines 8, 84. http://dx.doi.org/10.3390/machines8040084.